ELSEVIER

Chemical Engineering Journal 84 (2001) 173–192

Chemical Engineering Journal

www.elsevier.com/locate/cej

Review

Electrostatic enhancement of coalescence of water droplets in oil: a review of the current understanding

John S. Eow[a], Mojtaba Ghadiri[a,*], Adel O. Sharif[a], Trevor J. Williams[b]

[a] *Department of Chemical and Process Engineering, University of Surrey, Surrey, Guildford GU2 7XH, UK*

[b] *Electrical Power Engineering Research Group, Department of Electronics and Computer Science, University of Southampton, Southampton SO17 1BJ, UK*

Received 5 May 2000; accepted 21 October 2000

Abstract

This paper reviews the current understanding of electrocoalescence of water droplets in oil, highlighting particularly the mechanisms proposed for droplet–droplet and droplet–interface coalescence under the influence of an applied electric field, as well as various factors influencing the electrocoalescence phenomenon. Generally, the coalescence behaviour can be described in three stages: droplets approaching each other, the process of film thinning/drainage, and film rupture leading to droplet–droplet coalescence. Other possible mechanisms, such as droplet chain formation, dipole–dipole coalescence, electrophoresis, dielectrophoresis and random collisions, are also presented. Experimental work and mathematical modelling of the coalescence process are both reviewed, including various models, such as molecular dynamic simulation, random collision/coalescence modelling, and linear condensation polymerisation kinetics. The type of electric field, such as alternating, direct and pulsed direct current, plays a significant role, depending on the design and set-up of the system. The concept of an optimum frequency is also discussed here, relating to the electrode design and coating. Other factors, such as the average droplet size and the residence time of the liquid mixture exposed to the electric field, are highlighted relating to coalescence efficiency. The characteristics of the emulsion system itself determine the practicality of employing a high electric field to break the emulsion. Emulsions with high aqueous phase content tend to short-circuit the electrodes and collapse the electric field. Type and concentration of surface-active components have been shown to impart considerably stability and rheological property changes to the interfacial films, thus making the coalescence mechanism more complicated. More investigations, both experimental and by computer simulation, should be carried out to study the electrocoalescence phenomenon and to contribute to the design and operation of new electrocoalescers.

Keywords: Electrostatic separation; Coalescence; Droplet–droplet interaction; Film drainage; Film rupture; Water-in-oil emulsion; Collision; Surfactants

1. Introduction

To date, there exist several techniques for enhancing the separation of water-in-oil emulsions, such as the addition of chemical demulsifier [1], pH adjustment [2], gravity or centrifugal settling [3], filtration [2], heat treatment and electrostatic demulsification [4,5]. From the viewpoints of energy efficiency, electrical demulsification is considered to be the best among the above methods [4].

The electrical phase separation concept has been used in the petroleum industry for separating water-in-crude oil dispersions by applying a high electric field onto the flowing emulsion to effect flocculation and coalescence of dispersed water droplets [6,7]. Bailes and Larkai [8,9] applied this technique to promote phase separation of an aqueous dispersion from an organic phase, and developed an effective separator for solvent extraction. Some coalescence can occur due to Brownian motion and differential sedimentation, but these effects are insignificant compared to electrocoalescence [10]. Generally, an irreversible rupturing of the emulsions can occur in an electric field due to the coalescence of droplets [11]. In low electric fields, however, water droplets attain a linear chain-like configuration, though the electric field is not high enough to induce coalescence. When the field is switched off, the droplets return to a random distribution [12,13].

The concepts here are believed to be the interaction between the drops and the externally applied electrostatic field, resulting in drop charging and agglomeration, and eventually coalescence. Generally, external electric fields can cause the coalescence of drops at an interface, and drop–drop coalescence in a dielectric fluid. When two drops approach

---

[*] Corresponding author. Tel.: +44-1483-879-470; fax: +44-1483-876-581.
E-mail address: m.ghadiri@surrey.ac.uk (M. Ghadiri).

1385-8947/01/$ – see front matter
PII: S1385-8947(00)00386-7

Nomenclature

a	film radius (m)
b	constant
C_c	conductivity of continuous phase (S/m)
C_d	conductivity of disperse phase (S/m)
C_DP	conductance of the dielectric phase (S)
C_m	medium conductivity (S/m)
C_s	conductivity of solid (S/m)
d	distance between closest surfaces of drops (m)
d_c	thickness of continuous phase (m)
d_d	diameter of a drop (m)
d_s	thickness of solid (Perspex) (m)
d_0	distance between drop centres (m)
d_2	thickness of aqueous phase (m)
d_{32}	Sauter mean particle or drop diameter (m)
e	eccentricity of the shape of a prolate spheroid
E	electric field strength (V/m)
E_c	critical electric field at the drop surface (V/m)
E_iz	applied electric field in the z-direction (V/m)
E_max	peak electric field strength (V/m)
$E_{r'}$	electric field of r-component in spherical coordinate (V/m)
E_θ	electric field of θ-component in spherical coordinate (V/m)
E_μ	potential energy of dipolar moment (J)
E_0	applied electric field (V/m)
E_1	the field inside the drop (V/m)
f_c	collision frequency (s^{-1})
f_N	mean drop collision frequency (s^{-1})
f_os	frequency of oscillator (Hz)
f_p	optimum pulse frequency (pulse/s)
F	the force attracting the two surfaces together (N)
F_e	the force of attraction on drops (N)
F_i	any possible force applied to the droplet i (N)
F_i^hyd	hydrodynamic force on droplet i (N)
$F_i^\mathrm{rep}(\mathrm{h})$	the short-range repulsive force between droplet i and the electrode (N)
$F_{ij}^\mathrm{el}(R_{ij}, \theta_{ij})$	induced dipole–dipole interaction between droplet i and droplet j (C m)
$F_{ij}^\mathrm{rep}(R_{ij})$	the short-range repulsive force between any two droplets (N)
g	acceleration due to gravity ($\mathrm{m\,s^{-2}}$)
G	capacitance of two adjacent droplets (F)
G_DP	capacitance of the dielectric phase (F)
h	thickness of film (m)
h_0	initial film thickness (m)
I_m	mean conduction current (A)
J_{ij}	rate of collision per volume of drops of size i with drops of size j ($\mathrm{s^{-1}\,m^{-3}}$)
k'	proportionality constant in Eq. (10.1) ($\mathrm{s^{-1}\,kV^{-0.5}\,m^{-3}(Pa\,s)^{3.2}}$)
K_c	collision coefficient
K_d	demulsification rate constant (defined by Eq. (10.1) (s^{-1})
K_dif	coefficient of diffusion ($\mathrm{m^2/s}$)
K_P1	proportionality constant
K_P2	proportionality constant
$K_\mathrm{R,2}$	second-order rate constant
K_1, K_2, K_3	coefficients
L_e	distance between the electrodes (m)
m_d	mass of each droplet in emulsion (kg)
m_1	ratio of first drop radius to the distance between drop centres
m_2	ratio of second drop radius to the distance between drop centres
n	length of chain (m)
n_i	number of drops of size i per unit volume (m^{-3})
n_p	number of particles per unit volume (m^{-3})
$N(w, t)$	number of drops of volume w per unit volume (m^{-3})
N_0	initial number of droplets
p	distance defined in Fig. 3 (m)
P	probability that a droplet has formed two attachments
$P^{(1)}$	pressure inside a drop (Pa)
$P^{(2)}$	pressure outside a drop (Pa)
q_d	double-layer charge of a drop (C)
q_i	charge of a drop due to contact charging (C)
r	droplet radius (m)
r'	spherical coordinate (radial) (m)
r_c	radius of the circle of contact resulting from deformation (m)
r_2	second droplet radius (m)
R_i	radial position of droplet i (m)
ΔR_i	radial displacement of droplet i (m)
t	time (s)
t_f	fall-time of pulsed d.c. waveform (s)
t_off	‘off’ time of pulsed d.c. waveform (s)
t_on	‘on’ time of pulsed d.c. waveform (s)
t_r	rise time of pulsed d.c. waveform (s)
t_1	characteristic time (s)
U_int	interfacial velocity (m/s)
U_T	terminal velocity of a drop (m/s)
$U_i^{(0)}$	velocity of size i drops due to gravity only (m/s)
V	electric potential (V)
V_p	electric potential induced on the surface of the Perspex (V)
V_s	potential of sphere (V)

V_0	the applied potential (V)
y	separation between two droplet surfaces (defined in Fig. 3) (m)

Greek symbols

α	polarisability of water droplets (F m^2)
β	correction for the value of the permittivity of a mixture
γ_0	dimensionless parameter
δ	adsorbed layer thickness (m)
δ_{DL}	double-layer thickness (m)
$\Delta\rho$	density difference between aqueous and organic phases (kg/m^3)
ε_0	permittivity of vacuum (F/m)
ε_1	dielectric constant of continuous phase
ε_2	dielectric constant of aqueous phase
ε_{m}	dielectric constant of emulsion
ε_{s}	dielectric constant of solid
ζ	zeta-potential of particles (V)
η_{c}	viscosity of continuous phase (Pa s)
θ	spherical coordinate (angular) (rad)
λ	oil/water interfacial tension (N/m)
μ	dipole moment (C m)
ρ	mass density (kg/m^3)
ρ_{c}	density of continuous phase (kg/m^3)
σ	approach distance of a drop to an interface (m)
τ	charge relaxation time (s)
$\tau_{\mathrm{M–W}}$	the Maxwell–Wagner time constant (s)
$\tau_{\mathrm{R\text{-}T}}$	average rest-time of droplets at interface (s)
ϕ	water hold-up or volume fraction of emulsion
ϕ_{l}	the local volume fraction of the dispersed phase
ϕ_{p}	packing factor
ψ_1(h/b)	function defined by Eq. (9.6b) describing a geometrical factor
ω	hyperbolic cosine of $(h/b+1)$

each other, the interface is separated by a thin film of oil determining emulsion stability. Thus demulsification requires rupturing of this interfacial film [14]. Generally, the main purposes of an applied electrical field are to promote contact between the drops, to help in drop–drop coalescence, and to encourage drop–interface coalescence. However, coalescence may also cause phase inversion of emulsions [15]. Water-in-oil emulsion stability can be assessed by several techniques such as the 'bottle test', turbidity measurements [16], time-domain dielectric spectroscopy (TDS) [17] and the differential scanning calorimetry (DSC) technique [18]. Stability of water-in-oil emulsions in high electric fields can be investigated by the TDS technique [11].

Efforts to apply this technology directly to other liquid phase separations such as solvent extraction, where the proportion of the aqueous phase is usually much higher [19,20], have been hampered by bridging of the electrodes by the more conductive aqueous phase. The efficiency of electrical process is usually related to power consumption. A very small amount of current would be drawn for a completely insulating oil. The main factors influencing the consumption of power practically will therefore be the conductivity of the continuous phase and bridging of the electrodes.

There have been few developments in the fundamental knowledge of electrocoalescence fundamental principles and governing factors, with most attention being given to the design of new coalescers. A complete fundamental understanding and comprehensive prediction of the coalescence of drops in an electric field is lacking because of the complexity of the electrostatic and hydrodynamic interactions, as well as the difficulty in defining the electrical field strength that is actually experienced by the drops.

A greater understanding of the processes taking place during the water/oil emulsion separation in an electric field, especially the actual coalescence process, should provide the knowledge for optimum design of the electrode geometry and the type of electric field. It can also reduce the residence time in order to minimise the size and weight of the equipment. The state-of-the-art in the current understanding of drop–drop and drop–interface coalescence, as well as the various aspects of the electric field itself are reviewed here, thus directing us towards a greater understanding of the mechanisms of electrocoalescence.

Table 1 shows details of the past work concerning electrical phase separation for water-in-oil type emulsions. Fig. 1 summarises the mechanisms and factors influencing the coalescence efficiency of aqueous-drop-in-oil dispersions.

2. Mechanisms and models of coalescence

Cottrell and Speed [6] filed the first patent on electrocoalescence, observing the coalescence mechanism when a high potential was applied to a pair of wire electrodes in an aqueous-in-oil emulsion. Chains of aqueous drops extended from one electrode to the other. Coalescence of adjacent drops in each chain then occurred and the drops next to the electrodes became larger as new drops were acquired by the chain. Almost any type of high electric field will assist the separation of water-in-oil dispersions to some extent [40]. The mechanisms for this phenomenon are however not yet clearly understood [41] other than the electrical forces facilitate the coalescence between small drops in order to attain suitable drop sizes rapidly for gravity separation. However, possible mechanisms have been proposed for the separation of emulsion in an electric field, as shown in Fig. 1, involving such effects as chain formation, dielectrophoresis, electrophoresis, formation of intermolecular bonds, dipole coalescence, electrofining and random collisions [42,43].

Table 1
Electrical phase separation for water-in-oil type emulsions

Investigator	Type[a]	Apparatus[b]	Electrode[c]	Continuous phase	Dispersed phase (hold-up, vol. %)
Charles and Mason [21]	B	CV	CP; d.c.	Heptane	Water (single drop)
Bailes and Larkai [8,9]	C	RD	CP; pulse d.c. (1, 1.5, 60 Hz)	Escaid 100-LIX64N	H_2SO_4 (saturated)
Ino et al. [22]	B	CV	GT; a.c.	Kerosene-Span 80–LIX64N	NaCl aq. sol.
Galvin [23]	C	RD	CP; pulse d.c. (1–10^3 Hz) and d.c.	Mix sol. — alamine 336	Water (50%)
Yamaguchi et al. [24]	C	Col.	BP; d.c.	Kerosene-Span 80	NaCl aq. sol.
Hsu and Li [25]	C	CV	CT; a.c.	Paraffin–Polyamine–D2EHPA	$FeSO_4$ aq. sol. (33%)
Kriechbaumer and Marr [26]	C	RD	CP; a.c.	Shellsol–ECA4360–LIX64N	$CuSO_4$ aq. sol. (14%)
Kataoka and Nishiki [27]	C	RD	BP; pulse d.c.	Kerosene-Span 80 — TOA, LIX64N	NaCl aq. sol., others
Mori and Eguchi [28]	B	RD	CP; a.c. (60–1800 Hz)	Dodecane — SP-010, ECA4360J	LiOH, HCl aq. sol.
Bailes and Stitt [29]	C	Col.	CT; pulse d.c. (4 Hz)	Isopar M	NMP + ethylene glycol (80%)
Yan et al. [30]	B	CV	CT; pulse d.c. (0.5, 5, 50, 500 Hz)	Kerosene — Polyamine TOA, others	NaOH aq. sol. (20, 70%)
Kumar et al. [31]	C	Col.	CT; pulse d.c. (1–100 Hz)	Escaid 100-LIX64N	Cu aq. sol. (25, 50%)
Taylor [32]	B	Microscopic cell	GT; a.c.	Crude petroleum oil	Distilled water (5%)
Hano et al. [33]	C	CV	CT; a.c.	Kerosene-Span 80, others	$CuSO_4$ aq. sol., others (50%)
Goto et al. [4]	C	TV	CP; a.c.	Kerosene-Span 80 — LIX64N, others	$CuSO_4$ aq. sol., others
Hauertmann et al. [34]	C	RD	CP; a.c. (0.1–2 kHz)	Kerosene-Span 80 — D2EHPA, others	H_2SO_4 aq. sol.
Taylor [35]	B	Cylindrical microscopic cell	GT; a.c.	Dry, export grade Kuwait crude oil	Double-distilled water containing 0–0.5 M (4%) AnalaR sodium chloride
Hirato et al. [36]	B	TV	BP; d.c.	Kerosene	Na_2CO_3 aqueous (50%)
Chen et al. [37]	B	Microscopic stage cell	BP; a.c. (1–50 Hz)	Buchan crude oil	Water (20%)
Williams et al. [38]	C	RD	CP; a.c.	Gas oil	Water (4.5%)
Taylor [39]	B	Microscopic stage cell	CP; a.c. (1–300 Hz) and pulsed d.c. (1–200 Hz)	Jet A1 kerosene	Water (10–20%)
Figueroa and Wagner [20]	B	CV	CT; a.c. (2000 Hz); pulsed d.c. (600 Hz)	Guayule resins dissolved in xylene	Distilled water (25–50%)

[a] B: batch demulsification; C: continuous demulsification.

[b] Col.: Column (vertical direction); CV: circular vessel (with radial flow); RD: rectangular duct; TV: tubular vessel (horizontal direction).

[c] BP: bare plate; CP: coated plate; CT, coated tube; GT: glass tube; a.c.: alternating current (at mains frequency, unless stated); d.c.: direct current.

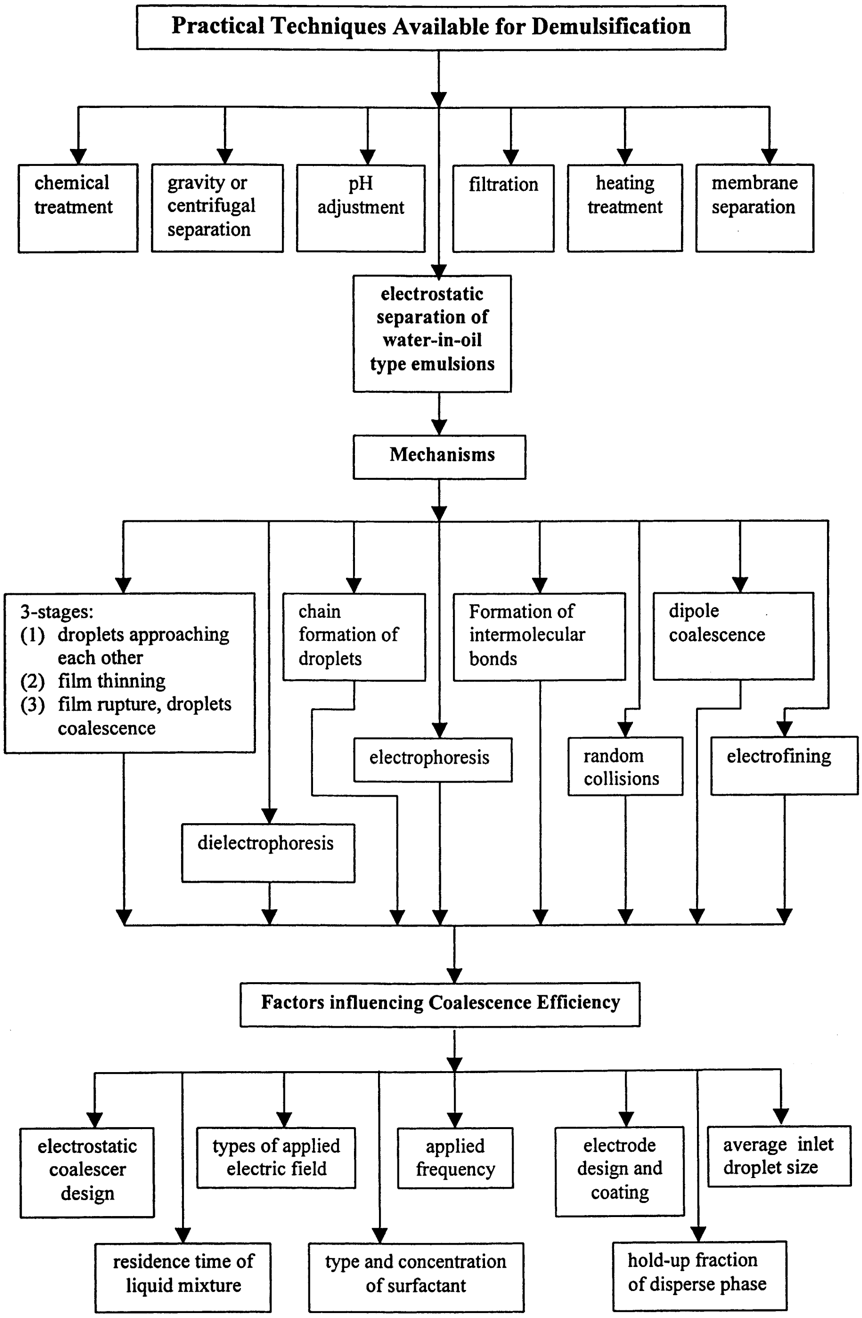

Fig. 1. Mechanisms and factors influencing the coalescence efficiency of electrostatic separation of water-in-oil type dispersions.

The dominant mechanisms should depend on factors such as the fractional volumetric hold-up of dispersed phase, electrode geometry and type of electric field although they have not been studied systematically. Two mechanisms for the electrocoalescence of water drops in electric fields, i.e. dipole–dipole coalescence and ‘electrofining’ have been described by Waterman [44]. ‘Electrofining’ covers electrophoresis, dipole coalescence, collision of oppositely charged drops moving in opposite directions and collisions of different sized drops moving in the same direction for d.c. electric fields [44].

In an a.c. electric field, Galvin [23] observed that coalescence occurred between pairs of drops rather than through chain formation of drops, with the approach speed increasing with decreasing drop–drop separation, and there appeared to be no film resistance to coalescence. Deformation of the drops occurred before coalescence. A rigid sphere model was suggested although the coalescing surface radius would be less than that of the drop. According to Galvin [23], electrophoresis could not be an important mechanism here, as coalescing drops preferred to move in opposite directions with similar velocities. Gravitational separation of the enlarged drops then follows, as governed by the Stokes' equation:

$$U_{\mathrm{T}} = \frac{2r^2 \Delta\rho g}{9\eta_{\mathrm{c}}} \tag{2.1}$$

Therefore, from Eq. (2.1), it is clear that intensification of sedimentation results from increasing the drop size, increasing the density difference between the phases and increasing the continuous phase viscosity. The density difference and viscosity of the phases can be controlled by diluents and temperature, respectively [45], whereas the drop size can be controlled by applied electric field. It is therefore the applied electric field that controls the efficiency of a given system.

Eq. (2.1) is only valid for a single particle, away from any wall, and assumes the non-slip boundary condition. Modification is needed to account for a particle near a wall, multiple particle settling (especially if not monodisperse), and circulation of the internal phase if the particle is a liquid. The Rybczynski–Hadamard equation [46], which predicts 50% faster settling speeds in some cases, accounts for the latter point. However, the non-slip boundary condition may still be applicable if surfactant renders the interface immobile. Nevertheless, the important point is that settling speed is proportional to the square of drop size which shows the great importance of coalescence prior to phase separation.

2.1. 3-Stage process/mechanism

The coalescence between drops in an immiscible liquid medium, or between a drop and its own bulk phase occurs in three stages [3,12,43,47]. In the first stage, the drops approach each other and are separated by a film of the continuous phase. The second stage involves the thinning of this film to reduce the interfacial area. The thinning rate is affected by the capillary pressure and disjoining pressure, and can be retarded due to the Marangoni effect if surfactant is present [41,48]. With high shear rate, the film thinning rate is inversely proportional to the square of drop size [14]. When the film reaches a certain critical thickness, any significant disturbance or instability will cause it to rupture, and coalescence occurs [41,49]. Film thinning is often the overall controlling step. Rommel et al. [48] and Manev et al. [50] studied the thinning rate of aqueous foam films, and considered it to be influenced by surface diffusion of soluble surfactants in bulk phases.

2.2. Dipole coalescence

For dipole coalescence to take place, droplets have to be brought together by various ways, such as Brownian motion, sedimentation, flocculation and electrophoresis, with laminar or turbulent flow mixing being generally the most important mechanisms when there is fluid flow. The classical equation for dipole–dipole interaction between two similar spherical particles/drops gives the electrostatic force as

$$F = \frac{24\pi \varepsilon_0 \varepsilon_1 r^6 E^2}{(d+2r)^4} \tag{2.2}$$

where ε_0 is the permittivity of vacuum, ε_1 the dielectric constant of the continuous phase, d the distance between the near surfaces of the two drops, E the electric field strength and r the drop radius [44]. Williams and Bailey [10], Bailes and Stitt [29] and Waterman [44] considered this force to be the principal cause of coalescence in a.c. and d.c. electric fields. It is worth noting that Eq. (2.2) is only a first-order approximation to the actual force which relies on polarisation effects and is short range. It becomes invalid when the drops get closer together than a certain critical distance which depends on drop size. In this case, higher-order terms must be considered. The force expression, which is dielectrophoretic in nature, assumes that the drops are uncharged and of equal size. Further, droplet deformation, which occurs in the presence of a strong electric field, is ignored.

According to Williams and Bailey [10], electrostatic coalescence is a combination of dipole coalescence and 'migratory coalescence'. Dipole coalescence is due to a dielectrophoretic attractive force between two water drops, from their polarisation in the electric field. Migratory coalescence is electrophoretic, relying on the drops being charged. A drop may initially possess electric double-layer charges, as given in

$$q_{\mathrm{d}} = \frac{4\pi r^2 \varepsilon_1 \varepsilon_0 \zeta}{\delta_{\mathrm{DL}}} \tag{2.3a}$$

where the double-layer thickness

$$\delta_{\mathrm{DL}} = \left(\frac{K_{\mathrm{dif}} \varepsilon_1 \varepsilon_0}{C_{\mathrm{m}}}\right)^{1/2} \tag{2.3b}$$

where ζ is the zeta-potential of the drop, K_{dif} the coefficient of diffusion and C_{m} the conductivity of the continuous medium [10]. Further charging can occur, by contacting an electrode [10] as in

$$q_i = \left(\frac{\pi^2}{6}\right) 4\pi r^2 \varepsilon_1 \varepsilon_0 E_0 \tag{2.4}$$

Also drops must retain their charges sufficiently long to traverse the distance between the electrodes in the electric field. Electrophoresis, arising from the electrostatic attraction of charged electrodes for charged drops [51], moves the drops in the electric field direction. Migratory coalescence, which usually occurs in a unidirectional field as the direction of droplet motion is fixed, relies on the charge relaxation time τ being long [10]

$$\tau = \frac{\varepsilon_1 \varepsilon_0}{C_{\mathrm{m}}} \tag{2.5}$$

Zhang et al. [52] believe that an external electric field, no matter how small, induces charges of opposite sign on the closest surfaces of two aqueous drops. When two drops are close to each other, the presence of the neighbouring drop affects the potential field around the other drop. This causes an additional hydrodynamic resistance on each drop, resulting in the drops flowing around one another. If two drops are sufficiently close, van der Waals attraction may also become important [52], helping to pull nearby drops into contact and holding them together during coalescence, due to the tendency of interfacial tension to minimise the surface area.

The main effect of an aqueous drop in a dielectric will be polarisation from reorientation of induced dipoles with respect to the external electric field. The magnitude and direction of the electric field induced force between two drops vary with the orientation of the external electric field relative to the line-of-centres of the two drops.

When relatively conducting water droplets, dispersed in a dielectric oil, are subject to an external electric field, the re-distribution of droplet surface charges will create interfacial polarisation of the droplets [37], and induce dipole moments in them. This induced dipole moment in an a.c. electric field is given by [53,54]:

$$\mu = \alpha E \tag{2.6a}$$

where μ is the induced dipole moment and α the polarisability of the water droplets.

$$\alpha = \tfrac{1}{2}\pi \varepsilon_0 \varepsilon_1 d_\mathrm{d}^3 \beta \tag{2.6b}$$

$$\beta = \frac{\varepsilon_2 - \varepsilon_1}{\varepsilon_2 + 2\varepsilon_1} \tag{2.6c}$$

2.3. Film thinning/drainage

The strength of the interfacial film of oil between water droplets is very important in a water/oil emulsion [41], with the life-time of the film determined by two processes; thinning and breaking. Film thinning occurs by drainage of the liquid under gravity and suction at the plateau-borders. When the thickness is reduced to about 1000 Å, other surface forces influence the drainage; van der Waals attraction increases the drainage rate; double-layer repulsion decreases it [41,55,56]. Further thinning will cause some films to become metastable. Metastability occurs when border suction, van der Waals attraction and double-layer repulsion are balanced; instability results when the attraction forces predominate, due to external disturbances such as thermal shocks, vibration and particles. Higher surfactant concentrations can also produce a lower demulsification rate [1]. The life-time and critical thickness of an unstable film have been calculated by Vrij [55], assuming a laminar liquid flow between rigid film surfaces at a constant velocity.

Charles and Mason [57], Allan and Mason [58] and Brown and Hanson [59] concluded that drop–interface coalescence in an electric field occurs by the film drainage mechanism but that it is accelerated due to the electrical force on the drop at the interface. When the drops are within a critical distance of one another, the film separating them can rupture rapidly, followed by drop–drop coalescence [52]. This occurs when the electric field between the two drops has attained the dielectric breakdown strength of the surrounding fluid. The liquid film can also succumb to an electrohydrodynamic instability. Equations for drop deformation, film thinning rate, and film rupture and collapse have been given by Charles and Mason [57]. Bailes and Kalbasi [60] have shown that charged drops, outside an electric field, tend to have a coalescence behaviour similar to that of uncharged drops in an electric field.

The angle of drop–drop coalescence and contact time are observed to reduce with increasing field strength up to instantaneous coalescence [61], the electric field enhancement being responsible for the rupture of the interfacial film. Allan and Mason [61] and Sartor [62] suggested that in a d.c. electric field the film separating the two drops breaks down as the drops approach each other; coalescence is then initiated by puncturing due to spark discharge. Williams et al. [38] and Harpur et al. [63] are of the same view but believe that the initial approach is generally caused by turbulent mixing, as the electrostatic attraction, due to polarisation between drops, is short range.

2.4. Chain formation and the coalescence mechanism

A two-step mechanism of chain formation and coalescence for water-in-oil dispersions has been proposed, which is influenced by a number of factors, including oil phase viscosity, disperse phase volume and the applied electric field strength [35]. This mechanism has been observed with both d.c. and a.c electric fields. Chains of drops are formed by movement of single drops, with the chains aligned in the direction of maximum field strength. Moreover, the chains do not always start or finish at an electrode and may not be in contact with the electrodes.

Pearce [64] suggested that chains are formed by forces due to the potential difference between drops as a result of their induced charges. However, Bezemer and Goes [65], using an emulsion with water content of only 0.1%, observed that chains were only formed after a long time and that there was a movement of drops in the direction of maximum field strength, suggesting an additional dielectrophoretic force (see Section 2.6). The actual coalescence process depends on two factors, i.e. the dielectric breakdown of the continuous phase film between adjacent drops, and the attractive force between drops due to their potential difference. The film may also rupture by other means than electrostatic breakdown.

For stationary emulsions, Taylor [32,35] has shown that stable chains of drops will be created if the drops are surrounded by a rigid interfacial film, eventually leading to the bridging of the electrodes. Mohammed et al. [66] revealed that asphaltenes form solid films, retarding the film drainage rate between two water drops. The drops will deform into an ellipsoidal shape [23] owing to the induction of a dipole [37] and redisperse into the continuous phase, due to the interaction between interfacial tension and the electric stresses [44]. Taylor [32] reports two distinct types of behaviour. In type I, very stable droplet chains form between the electrodes, on the application of an a.c. electric field, resulting in current leakage through the chains. Drop–drop coalescence is prevented by rigid interfacial films. However, with the addition of an oil-soluble surfactant, the type I characteristics transforms to type II, where rapid droplet coalescence occurs, indicating the lack of any chain formation and enhanced mobility of the interfacial film. Without a rigid film, the neighbouring droplets tend to stick together and coalesce to form larger drops in an electric field. Thus, coalescence is more likely to occur before chain formation when the interfacial film is compressible.

2.5. *Electrophoresis*

The term 'electrophoresis' refers to the movement of a charged particle through a stationary fluid under the influence of an electric field [67]. The fundamental principle here is the charge separation between the particle surface and the fluid immediately surrounding it. An applied electric field acts on the resulting charge density, causing the particle, the fluid around the particle or both to move. The electrophoretic mobility is defined as the particle velocity divided by the strength of the electric field [41].

2.6. *Dielectrophoresis*

'Dielectrophoresis' is defined as the motion of matter caused by polarisation effects in a non-uniform electric field [68]. For drops with a permittivity greater than that of the suspension medium, as in the case of water drops in oil, they move toward the place of greatest field intensity. This does not require charged particles and it depends on the force felt by all polar materials when in a non-uniform electric field. Any dipole will have a finite separation of equal amounts of positive and negative charges in it and the electric field will be in alignment with the dipole. As the field is non-uniform, one end of the dipole will be in a weaker field, resulting in a net force, pulling the dipole towards the place of greatest field intensity. The direction of the field can be reversed and this still gives rise to the original direction of the dipole travel as the force is dependent on the square of the electric field strength. In most practical situations, the contribution of dielectrophoresis may be small as compared to electrophoresis, as the velocity of a droplet due to the dielectrophoretic force is relatively low in a highly divergent electric field [23,51].

However, it should be noted that dipole coalescence is a manifestation of dielectrophoresis; a pair of water drops in oil, of small separation, are attracted to one another and each can be thought of as striving to reach the point of maximum field intensity between the drops. As the inter-drop separation reduces, the dipole approximation becomes invalid and higher-order terms must be considered which account for the greatly increased interaction at very small separations. Dielectrophoresis can even occur when the applied electric field is spatially uniform as a result of the field perturbations caused by the presence of the drops. In situations where the drops are unlikely to be significantly charged, such as when a.c. excitation or insulated electrodes are used, dielectrophoresis is of prime importance with regard to coalescence.

3. Mathematical modelling of drop–drop and drop–interface coalescence

Hydrodynamic models for the separation of one liquid from another liquid at a horizontal liquid–liquid interface are given by Rommel et al. [48]. There are two major approaches in addressing the phenomenon: the 'deterministic models' focus on the drainage of a thin layer between a drop and an interface or between two neighbouring drops, and 'probability models' which consider the separation to be a stochastic process under the assumption of distinct probabilities of drop–drop coalescence and drop–interface coalescence. Most models calculate either the drainage time of a thin layer between two approaching interfaces, until rupture, or the approaching velocity between two drops or a drop and a plane interface. In addition, some models use dimensional analysis to evaluate the coalescence time [48].

It is possible to consider an electrostatic coalescer as one component in an electrical circuit [69,70], the dynamic response of which depends upon the relative influence of all effective elements. Bailes [70] suggested that during the 'on' period (when the applied voltage is on) charge separation occurs within the oil layer. When the upper electrode is charged positively, the negative charge carriers will move towards the upper electrode and the positive charge carriers will move towards and accumulate at the lower electrode. When the applied electric field is switched off, the system discharges like a heterogenous electret, with the upper and lower electrodes reduced to zero potential before the charges held within the oil begin to move. The surface of the dielectric layer may be regarded as an equipotential surface with zero potential. Consequently, all lines of force originating on the charges within the dielectric, and which do not terminate on similar charges, must terminate on the dielectric surface.

Taylor [35] employed a statistical analysis of the droplet chain formation process using linear condensation polymerisation kinetics. The number of x-droplet chains is given by Eq. (3.1):

$$N_x = N_0(1-p)^2 p^{x-1} \tag{3.1}$$

where N_0 is the initial number of droplets, assuming that at time t the probability that a droplet has formed two attachments is p. The number of chains with length (n) greater than x is given by Eq. (3.2):

$$N_{n>x} = \frac{N_0(p^2-1)p^{x-1}}{\ln p} \tag{3.2}$$

By considering droplet–droplet interactions to be of second-order kinetics, Eq. (3.3) is generated giving the probability of a drop forming two attachments.

$$p = \frac{N_0 K_{\mathrm{R},2} t}{1 + N_0 K_{\mathrm{R},2} t} \tag{3.3}$$

Video-microscopic examination of pulsed d.c. electric fields on water-in-kerosene emulsions [39] suggests that: (i) droplet–droplet attraction and coalescence occur on the rise and fall parts of the pulse sequence; (ii) it is frequency dependent, with coalescence rate exhibiting an optimum frequency; (iii) the process is affected by electrode insulation and the continuous oil phase.

Expressions for the collision frequency, f_{c}, can be derived if the drops are assumed spherical and follow the basic continuous phase flow [71]. For equal-size drops, f_{c} is given by Eq. (3.4):

$$f_{\mathrm{c}} = K_{\mathrm{c}} U_{\mathrm{c}} d^2 n_{\mathrm{p}}^2 \tag{3.4}$$

where U_{c} is the velocity of the continuous phase and d the distance between two drops. In reality, drop trajectories deviate significantly from the flow streamlines as each drop disturbs the flow in its vicinity.

Bailes and Larkai [9,40] derived a model based on a random collision/coalescence mechanism using an energy balance between the electrical energy consumption and the mechanical work done during coalescence. This allows the derivation of a mean drop collision frequency f_N, as given by Eq. (3.5):

$$f_N = \frac{I_{\mathrm{m}} L_{\mathrm{e}}}{2.89 \varepsilon_1 \varepsilon_0 V_{\mathrm{c}} E_{\max} \phi_1 [(\phi_{\mathrm{p}}/\phi_1)^{1/3} - 1]} \tag{3.5}$$

The drops are assumed to be uniform, and their spatial distribution is characterised by the packing term ϕ_{p}. The concentration of drops would cause them to re-distribute into a rhombohedral configuration with a constant packing factor of 0.74. This is justifiable at a drop hold-up of 50% or more, but for a smaller hold-up the packing factor will alter.

A molecular dynamics simulation was applied by Chen et al. [37] to investigate the behaviour of water-in-oil dispersions under an a.c. electric field, examining long-range and short-range interactions on the reorientation of water droplets. Electrostatic, thermal (Brownian) and hydrodynamic forces need to be considered for the long-range interaction. Also described are the interactions between droplets with rigid films at short range, with drop–drop coalescence occurring without these films. The movement of a drop can be described by an equation of motion [37], such as Newton's equation for droplet i given by Eq. (3.6):

$$m_{\mathrm{d}} \frac{\mathrm{d}^2 R_i}{\mathrm{d}t^2} = \sum F_i(R_i) \tag{3.6}$$

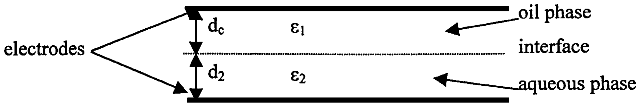

Fig. 2. The system used by Brown and Hanson [59].

For very slow motion of a microsized spherical droplet through an incompressible fluid, the 'creeping flow' model is appropriate, with the inertial force neglected compared to the viscous force. Thus the equation of motion can be simplified by setting the left-hand side of Eq. (3.6) to zero. Furthermore, the hydrodynamic force can be represented by a drag force as in Eq. (3.7) [74].

$$F_i^{\mathrm{hyd}} = -3\pi\sigma\eta_{\mathrm{c}} \frac{\mathrm{d}R_i}{\mathrm{d}t} \tag{3.7}$$

According to Chen et al. [37], the relation for the movement of water drops in oil under an a.c. electric field is similar to Klingenberg's equation [72], as shown by Eq. (3.8):

$$\Delta R_i^* = \left[\sum_{j\neq i} F_{ij}^{\mathrm{el}^*}(R_{ij}, \theta_{ij}) + \sum F_{ij}^{\mathrm{el}^*}(R'_{ij}, \theta'_{ij}) + \sum_{j\neq 1} F_{ij}^{\mathrm{rep}}(R_{ij}) + F_i^{\mathrm{rep}}(h) \right] \Delta t^* \tag{3.8}$$

where $*$ indicates a dimensionless variable. A system of two immiscible liquid phases between two platinum plate electrodes and with all the faces coplanar, as used by Brown and Hanson [59] is shown in Fig. 2.

A consideration of the electrostatic theory for this system leads to Eq. (3.9).

$$E_1 = \frac{3\varepsilon_2^2 V_0}{(\varepsilon_1 + 2\varepsilon_2)(\varepsilon_1 d_2 + \varepsilon_2 d_{\mathrm{c}})} \tag{3.9}$$

It does not consider the non-spherical nature of the drop at the oil–water interface, and also the very small amount of water dissolved in the oil, causing some power loss. It is further assumed that water behaves as a perfect dielectric; this is inaccurate and it is necessary to refine the above treatment to allow for the loss characteristics of water, thus yielding Eq. (3.10).

$$E_1 = \frac{3\varepsilon_2^2 (1 - \mathrm{j}\tan\delta)^2 V_0}{[\varepsilon_1 + 2\varepsilon_2(1 - \mathrm{j}\tan\delta)][\varepsilon_1 d_2 + \varepsilon_2(1 - \mathrm{j}\tan\delta) d]}, \quad \tan\delta \ \text{(the dielectric loss tangent)} = \frac{C_{\mathrm{DP}}}{2\pi f_{\mathrm{os}} G_{\mathrm{DP}}}, \quad \mathrm{j} = \sqrt{-1} \tag{3.10}$$

Substituting for $\tan\delta$ in Eq. (3.10) gives Eq. (3.11).

$$E_1 = \frac{3\varepsilon_2^2 (1 - \mathrm{j}(C_{\mathrm{DP}}/2\pi f_{\mathrm{os}} G_{\mathrm{DP}}))^2 V}{[\varepsilon_1 + 2\varepsilon_2(1 - \mathrm{j}(C_{\mathrm{DP}}/2\pi f_{\mathrm{os}} G_{\mathrm{DP}}))] [\varepsilon_1 d_2 + \varepsilon_2(1 - \mathrm{j}(C_{\mathrm{DP}}/2\pi f_{\mathrm{os}} G_{\mathrm{DP}})) d_{\mathrm{c}}]} \tag{3.11}$$

At low ionic strengths, G_{DP} is independent of frequency and so the measured value of $\varepsilon/\varepsilon_2$ is valid for values of f_{os} below 10 kHz. The term $\varepsilon/\varepsilon_2$ is sufficiently small to be neglected and so, to a first approximation, Eq. (3.11) reduces to Eq. (3.12).

$$E_1 = \frac{3V_0}{2d_c} \tag{3.12}$$

Allan and Mason [58] showed that the behaviour of the system is independent of the ionic strength of the aqueous phase, i.e. the aqueous phase may be considered to be perfectly conducting compared to the oil, without any potential drop across the aqueous layer.

The estimation of the drop–drop forces varies in complexity. For the self-capacitance of a conducting sphere of radius r adjacent to a grounded, conducting sphere of radius r_2 (where $m_1 = r/d_0$ and $m_2 = r_2/d_0$) with centres separated by a distance d_0, Eq. (3.13) due to Smythe [73] is given by:

$$G = 4\pi r\varepsilon_1\varepsilon_0\left[1 + \frac{m_1m_2}{1-m_2^2} + \frac{m_1^2m_2^2}{(1-m_2^2)^2 - m_1^2} + \cdots\right] \tag{3.13}$$

If the spheres have equal radius r then $m_1 = m_2 = r/d_0$. Smythe [73] also gives a more compact form of the self-capacitance, when the spheres have equal radius, involving hyperbolic functions. In the case of unequal sphere, Smythe [73] gives another expression for the self-capacitance in terms of hyperbolic functions. The force of attraction between the spheres under potential difference V_0 is given by Eq. (3.14) [73]:

$$F_e = 4V_0^2\pi\varepsilon_1\varepsilon_0\frac{r}{d_0} \times \left[\frac{m_1m_2}{(1-m_2^2)^2} + \frac{m_1^2m_2^2[2(1-m_2^2) - m_1^2]}{[(1-m_2^2)^2 - m_1^2]^2}\right] + \cdots \tag{3.14}$$

Taylor [39] has proposed another expression for the capacitance based on the work of Pearce [64], which differs slightly from Eq. (3.13), but it is incorrect.

In a uniform field E_0, the influence of the drop is equivalent to that of a dipolar moment μ at the drop centre [42]. Outside the drop, the electric potential V, is given by Eq. (3.15):

$$V(r',\theta) = \left[\frac{\mu\cos\theta}{4\pi\varepsilon_1\varepsilon_0 r'^2}\right] - E_0 r'\cos\theta \tag{3.15}$$

With the boundary conditions at the water/oil interface, we get for μ, V and the field components $E_{r'}$ and E_θ, the expressions given in Eqs. (3.16)–(3.18), respectively [42].

$$\mu = 4\pi\varepsilon_1\varepsilon_0 E_0 r^3 \tag{3.16}$$

$$V(r',\theta) = E_0 r'\cos\theta\left[\frac{r^3}{r'^3} - 1\right] \tag{3.17}$$

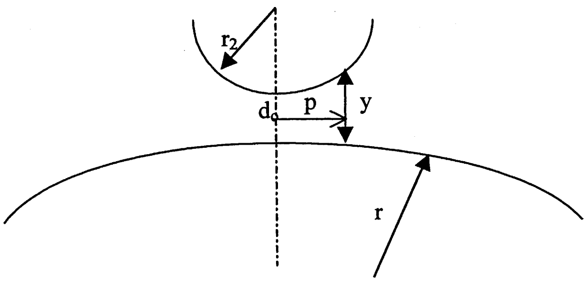

Fig. 3. Definition of d, p and y in the zone between two close drops (the axis joins the two drop centres).

$$E_{r'}(r',\theta) = E_0\cos\theta\left[1 + \frac{2r^3}{r'^3}\right] \tag{3.18a}$$

$$E_\theta(r',\theta) = E_0\sin\theta\left[\frac{r^3}{r'^3} - 1\right] \tag{3.18b}$$

In the case of two drops A and B of radius r and r_2, respectively ($r_2 < r$) with a large separation between their centres, the interaction force is given as $\mathbf{F} = -\nabla E_{\mathrm{U}}$, where E_{U} is the potential energy of the dipolar moment $\mu_{\mathrm{B}} = \alpha_{\mathrm{B}}E_0 = 4\pi\varepsilon\varepsilon_0 b^3 E_0$ in the field induced by dipole μ_{A}. The force components on drop B are given by Eqs. (3.19a) and (3.19b) which are valid only when the interaction of the drops is due to dipolar moments.

$$F_{r'} = -12\pi\varepsilon_1\varepsilon_0 r_2^3 E_0^2\left(\frac{r^3}{r'^4}\right)(3\cos^2\theta - 1) \tag{3.19a}$$

$$F_\theta = -12\pi\varepsilon_1\varepsilon_0 r_2^3 E_0^2\left(\frac{r^3}{r'^4}\right)\sin 2\theta \tag{3.19b}$$

When the distance $d (d = r' - r - r_2)$ between the drops is smaller than r_2 (the smaller radius) (see Fig. 3), the surface charge distributions on the drops are altered.

Davis [75] developed a treatment for two conducting spheres in a uniform field, obtaining Eqs. (3.20a) and (3.20b).

$$F_{r'} = -4\pi\varepsilon_1\varepsilon_0 r_2^2 E_0^2(K_1\cos^2\theta + K_2\sin^2\theta) \tag{3.20a}$$

$$F_\theta = -4\pi\varepsilon_1\varepsilon_0 r_2^2 E_0^2 K_3\sin^2\theta \tag{3.20b}$$

The three coefficients K_1, K_2 and K_3 are expressed as series depending on the ratios d/r_2 and r_2/r [75]. The few numerical values given by Davis [75] lead to a power law of the form $K_1 \sim d^{-\beta}$ with $\beta \approx 0.8$. The asymptotic expression of K_1 takes the empirical expression given by Eq. (3.21):

$$K_1(d) \to \left[\frac{1.25}{(1 + (r_2/2r))^4}\right]\left(\frac{r_2}{d}\right)^{0.8} \tag{3.21}$$

By comparing Eqs. (3.19) and (3.20), the transition between the two regimes tends to occur at $d/r_2 \approx 0.7$. Eqs. (3.20a) and (3.20b) will apply without major difficulty for small water volume fraction ϕ. For ϕ greater than about 10^{-3}

the problem is complicated. It is nevertheless possible to derive an expression for $F_{r'}$ by assuming that the potential difference between drops A and B is $\Delta V = (r + r_2 + d)E_0 \cos\theta$, as proposed by Atten [42].

Another assumption concerns the field value between the spheres (see Fig. 3): $E \approx \Delta V/y$, and in order to calculate the force, the spheres can be replaced by paraboloids of radius of curvature r and r_2. The force density is $\frac{1}{2}\varepsilon_1\varepsilon_0 E^2$ and by integration, we obtain Eq. (3.22):

$$|F_{r'}| \approx \pi\varepsilon_1\varepsilon_0\Delta V^2 \int_0^{r_2} \frac{p\,\mathrm{d}p}{y^2(p)} = \frac{\pi\varepsilon_1\varepsilon_0 E_0^2 \cos^2 r_2^2 (r + r_2 + d)^2}{d(2d + r_2 + r_\mathrm{d}^2/r)} \tag{3.22}$$

which for $d \ll r_2$, simplifies to Eq. (3.23):

$$|F_r| \approx \frac{\pi\varepsilon_1\varepsilon_0 E_0^2 \cos^2\theta (r + r_2) r r_2}{d} \tag{3.23}$$

Man et al. [47] employed a population balance model in an analysis of the transient drop size distribution.

4. Effects of the applied electric field

The predominant coalescence mechanisms in a system also depend on the nature of the applied electrostatic field. Alternating current (a.c.), the oldest and commonest configuration, is used extensively in resolving crude oil emulsions, while direct current (d.c.) is used in the treatment of low water content refined products, and a pulsed d.c. field with insulated electrodes is proposed for the treatment of high aqueous content emulsions [39].

In an electric field, the induced electrostatic force between two conducting drops is inversely proportional to approximately the fourth power of the separation distance between the drops [44]. Therefore, like the van der Waals force, the electric-induced force increases dramatically with decreasing separation between the drops and becomes important only when the drops are close to each other. However, this electric-induced force also increases with the square of the drop size, thus dominating the van der Waals force in the coalescence of large drops [52]. However, the field within the drop is not important with regard to coalescence. The coalescence rate improves as the applied electric field strength is increased.

Typically an electric field strength of around 100 V/mm [37] is used. If the strength becomes too high, various drop breakup mechanisms can occur [10], with four such mechanisms being identified, three of which are electrostatic, and the other hydrodynamic. A drop deforms into a thin thread under an electric field, and will burst into smaller drops if the field is too high, as the electric stress overwhelms the recovery force due to interfacial tension. This is supported by Nishiwaki et al. [77], who studied the deformation of droplets in an alternating electric field of frequency 60 Hz for drops of poly(propylene oxide) and water suspended in poly(dimethylsiloxane). The condition for drop stability is given by Eq. (4.1) [44]:

$$E_\mathrm{c} \le K_\mathrm{p1}\left(\frac{\lambda}{r}\right)^{1/2} \tag{4.1}$$

The critical field strength for droplet disintegration is given by Eq. (4.2) [39]:

$$E_\mathrm{c} = K_\mathrm{P2}\sqrt{\frac{\lambda}{\varepsilon_1\varepsilon_0 r}} \tag{4.2}$$

Above the critical field E_c, the interface becomes unstable and dispersion occurs, producing much finer droplets, with E_c given by Eq. (4.3) [42]:

$$E_\mathrm{c} = 0.64\left(\frac{\lambda}{2\varepsilon_1\varepsilon_0 r}\right)^{1/2} \tag{4.3}$$

These equations are all essentially the same but differ in their proportionality constants.

According to Miksis [76], the drop shape is determined by its dielectric constant and a dimensionless parameter γ_0 as given by Eq. (4.4):

$$\gamma_0 = \left(p^{(1)} - \frac{1}{8\pi}\rho\frac{\mathrm{d}\varepsilon_1}{\mathrm{d}\rho}(E_1)^2 - p^{(2)}\right)\frac{8\pi}{F^2} \tag{4.4}$$

For large γ_0, the drop is basically a sphere. As γ_0 decreases from infinity, the drop extends in the direction of the field. At first, it becomes nearly a prolate spheroid. As γ_0 decreases further, it elongates and retains its nearly prolate spheroidal shape if $\varepsilon_1 < \varepsilon_\mathrm{c}$, where ε_c is a certain critical value. However, if $\varepsilon_1 > \varepsilon_\mathrm{c}$, the drop will develop two obtuse-angled conical points at its ends, known as Taylor cones [78].

The effect of conductivity is very important in real dielectrics, concerning the effects of charge re-distribution for both the continuous and disperse phases [79]. Conductivity is more significant at low applied frequencies, as charge carriers can respond within the time-scale of the field changes. The establishment rate of a dipole on a drop surface will depend on the disperse phase relaxation time. The relaxation time of the continuous phase reflects charge retention by the drop. Equations have been derived for the current in the external circuit due to movement of conducting particles between electrodes [79], suggesting that it should be possible to achieve a significant reduction in the current by removing particle impurities from the continuous phase.

vThe combined use of different field types has also been applied for crude oil dehydration and desalting [80,81]. Generally, separation efficiency improves with increasing applied field strength [4]. Nevertheless, it has to be remembered that the opposite effect occurs at very high field strengths, i.e. drop break-up, depending on the physical and surface properties of the system, such as interfacial tension and bulk rheology. Furthermore, the effects of the electric field on system performance are not always consistent, due to variation of ionic species, solvent and surfactants used [82]. Therefore, the coalescence kinetics of water drops containing electrolytes coated by surfactants in organic solution has to be studied systematically.

The Hanai equation [83] relates the dielectric constant of the emulsion (ε_{m}), in the low-frequency limit, to the dielectric constant of the continuous phase (ε_1) and the volume fraction of the dispersed phase (ϕ):

$$\varepsilon_{\mathrm{m}} = \frac{\varepsilon_1}{(1-\phi)^3} \tag{4.5}$$

Eq. (4.5) is a limiting condition as the excitation frequency tends to zero. It also requires that $C_{\mathrm{d}} \gg C_{\mathrm{c}}$ and $C_{\mathrm{d}} \gg C_{\mathrm{m}}$, where C_{d} is the conductivity of the disperse phase, C_{c} the conductivity of the continuous oil phase and C_{m} the effective conductivity of the emulsion in the low-frequency limit. These conditions hold for an emulsion of water-in-oil type. With the above conductivity requirements (i.e. $C_{\mathrm{d}} \gg C_{\mathrm{c}}$ and $C_{\mathrm{d}} \gg C_{\mathrm{m}}$), the same equation is also true for the low-frequency limit of the effective emulsion conductivity if permittivity is replaced by conductivity.

4.1. Pulsed d.c. field

Bailes and Larkai [8,9], who used a pulsed d.c. electric field with insulated electrodes, concluded that a better efficiency could be attained for pulsed d.c. fields than for constant d.c. or a.c. fields. Thus, the concept of an optimum frequency was proposed, due to the dielectric properties of the electrode coating and the continuous phase. Bailes and Dowling [84] also established that a pulsed d.c. field applied to insulated electrodes is an efficient means for phase separation. They reported that coalescence rate is not only a function of pulse amplitude but also of its shape and frequency, with all these parameters having optimum values. The effects of pulse form (square, half-wave and triangular) on the parameters cannot, however, be stated accurately because the electrode insulation will certainly affect the pulse form. In fact, it largely eliminates the differences between the three forms of pulse, with half-wave and triangular pulses reducing to the same shape. The square pulse produced the highest strength electric field for a given applied voltage. The field strength across the dispersion can be estimated by Eq. (4.6) [19]:

$$E_0 = \frac{V_{\mathrm{p}}}{0.577 L_{\mathrm{e}}} \tag{4.6}$$

Bailes and Larkai [8,9,85] suggested that the varying rates of drop collision caused by the breaking and formation of drop chains are frequency dependent. Figueroa and Wagner [20] also obtained different responses for a.c. and d.c. fields. For pulsing d.c. fields, a linear function exists between separation rate and applied potential, though such a function is only appropriate for very high a.c. field frequencies. Microscopically, Taylor [39] observed some significant effects using a very low pulsation frequency of 0.1 Hz, consisting of four components: a rise component (rise time = t_{r}), an 'on' period (on-time = t_{on}), a fall component (fall-time = t_{f}) and an 'off' period (off-time = t_{off}), referring to Fig. 4. A square-wave-generated pulse has frequency-independent t_{r} and t_{f} [80] and a mark–space ratio (i.e. ratio of 'applied time-on' to 'rest-time off') of near-unity [40].

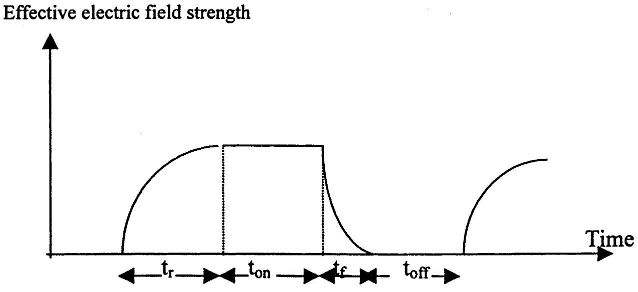

Fig. 4. Shape of a typical pulsed d.c. waveform [39].

During the rise time t_{r}, drops are observed to respond instantly, moving a short distance towards neighbouring droplets before coalescing upon contact [39]. During the remaining field application time, no further coalescence is observed. However, when the field is removed, further movement and coalescence is observed. No effect is observed during the off-time [39].

4.2. DC field

Using d.c. voltages from 5 to 25 kV with bare electrodes, Hirato et al. [36] showed that the demulsification percentage increases linearly with time until it reaches 60–70%, with both initial rate and maximum percent of demulsification increasing with applied potential. Bailes and Larkai [8] attributed the inefficient separation of the constant d.c. field to the leakage of the field strength or current through the insulating liquid. The problem is caused by interfacial polarisation and is described well by Galvin [23].

4.3. AC field

Hauertmann et al. [34] suggested that, with insulated electrodes, coalescence efficiency increases with field strength and frequency. However, Abou-Nemeh et al. [86] identified an optimum voltage-dependent behaviour in the region of 1 kHz using uninsulated electrodes. According to Taylor [32], the major effects of exposing dispersed water drops to high-strength a.c fields include drop deformation and drop–drop attraction, resulting from polarisation of the drops. These are different when d.c. fields are applied, establishing electrophoretic motions, which can lead to an increase in drop–drop collision rate. Furthermore, the behaviour of these emulsions in an a.c. field is said to depends on the crude oil type and chemical additives. Chains of drops are not formed when drop–drop coalescence occurs efficiently.

5. Effects of applied frequency

The flow of charge to and from the drops depends on the relaxation time of the various dielectrics, electrical properties of the continuous phase and the electrode coating material, and its thickness. For a pulsed d.c. field, the frequency affects the electrical relaxation of the inner surface of the electrode coating (Maxwell–Wagner effect), with the relaxation time and the optimum pulse frequency given by Eqs. (5.1) and (5.2), respectively [80,85]:

$$\tau_{\mathrm{M-W}} = \frac{(d_{\mathrm{s}}\varepsilon_{\mathrm{c}} + d_{\mathrm{c}}\varepsilon_{\mathrm{s}})\varepsilon_0}{(d_{\mathrm{s}}C_{\mathrm{c}} + d_{\mathrm{c}}C_{\mathrm{s}})} \tag{5.1}$$

$$f_{\mathrm{p}} = \frac{1}{2\pi\tau_{\mathrm{M-W}}} \tag{5.2}$$

Charge on a drop can travel to ground via the continuous phase. The relaxation time constant for this process is independent of geometry. In the case of insulated electrodes, the flow of charge in the insulation and that in the oil phase are also both independent of geometry. However, the relaxation time constant associated with the oil/insulator interface is dependent on geometry. This is why the Maxwell–Wagner time constant, involves the thicknesses of the oil and insulation layers. This time constant governs the electric fields in the system and the build-up of interfacial charge. Brown and Hanson [59], observing an optimum coalescence frequency for each system, suggested that vibrations and cavitation within the drop are responsible for the film rupturing, leading to coalescence of drops at an aqueous/oil interface. Moreover, they also suggested that it is the field inside the drop, rather than the charge it carries, that is responsible for enhancing the coalescence. They concluded that the electrical forces for coalescence are short range, and enhance film rupture. Therefore, the selection of the optimum frequency is very important, especially at low voltages, depending on the insulation material and its thickness, and liquid composition. Without insulation, the optimum frequency is determined by the electrical properties of the continuous phase. The mark/space ratio of the pulse is also important, as the 'time-on' should equal the 'time-off' for optimum coalescence [80,85]. However, Galvin [23] pointed out that the voltage rise and fall time constants of the electrical circuit were more important, these being determined by the electrical resistance of the circuit and the capacitance of the coalescer, recommending that the applied pulsed d.c. frequency should be within the range given by Eq. (5.3):

$$(2\pi\tau_{\mathrm{M-W}})^{-1} < f_{\mathrm{p}} < (2\pi\tau_{\mathrm{P-S\,rise}})^{-1} \tag{5.3}$$

Galvin [23] also agreed with Bailes and Larkai [85] that coalescence at low frequencies is independent of the electrode insulation. The r.m.s. potential value at the Perspex/organic interface varies in a predicted manner with applied voltage. The field strength shows a similar variation with the applied frequency. However, Galvin [23] believed that there is no fundamental reason why coalescence falls with increasing frequency, and that this may be due to limitations in the power supply circuit. His findings show that efficient coalescence is possible using an a.c. field at mains frequency, and he also gave an equation for the attractive force between two identical drops, the force being proportional to the square of the field strength.

It should be noted that although the coalescence efficiency increases with frequency at low frequencies (up to 10 Hz) as found by Bailes and Larkai [8,9,40], the performance is satisfactory up to 200 Hz, as limited by the rise time supply voltage [23]. This contradicts the results of Bailes and Larkai [8,9,40] who showed a sharp decrease in performance at applied frequencies above 10 Hz. At low frequencies, electrode insulation reduces the r.m.s. value of field strength due to the Maxwell–Wagner voltage decay [23]. If the coalescence behaviour exactly followed the field strength, much better coalescence would be expected at low frequencies without electrode insulation. Therefore, it seems unlikely that the frequency dependence (at low applied frequencies) is mainly due to the electrical circuit, suggesting a further effect must be present, possibly hydrodynamic. In flowing dispersions, there is always a degree of random mixing present. If the application of an electric field creates some kind of structure in the dispersion (e.g. droplet chains), the dispersion will return to its initial condition rapidly when the field is switched off.

Chen et al. [37] observed that at low frequency, long chains form between the electrodes. Higher frequencies caused the formation of shorter chains and led to coalescence. At frequencies up to 1 kHz, short chains of drops were formed, presumably as a result of the drops having insufficient time to respond to the rapidly changing current. Generally, the formation of chains is due to polarisation of the drops with respect to the external electric field [37]. Taylor [39] has also shown experimentally that there is an optimum frequency for maximum coalescence, depending to some extent on the applied voltage.

6. The effect of electrode design and coating

Considerations of electrode design and insulation type have been the subject of several investigations. Hsu et al. [87] reported good coalescence with a.c. fields using insulated electrodes with a hydrophobic surface. As expected, the thinner the coating, the better is the coalescence. Bailes and Larkai [9] supported the view that it is the interfacial relaxation between the insulation and the continuous phase that determines the way the drops are charged up. An optimum frequency could be obtained by a suitable choice of electrode coating material and thickness. The Perspex used by Bailes and Larkai [9] had a dielectric constant of 3.5, an electrical conductivity of 3.162×10^{-13} S/m and thickness of 6 mm. Teflon-coated stainless steel electrodes were used by Taylor [39]. Without electrode insulation, it is expected that only the continuous phase will determine the optimum frequency [9,80].

However, Galvin [23] dismissed claims by Bailes and Larkai [9] regarding the use of insulated electrodes to increase the separation efficiency, arguing that insulation serves just to prevent short-circuiting, and only increases the applied potential required to effect the same coalescence rate. Galvin [23] also recommended that if short-circuiting is a major problem, a current-limiting device should be applied so that electrode insulation is not required. However, according to Bailes and Larkai [9] and Bailes [80] the importance of electrode insulation is that, should bridging occur between the electrodes, the charge is only locally reduced at an insulated electrode surface. With bare electrodes, such bridging would discharge the full stored energy of the capacitor at the point of short-circuiting, and the whole electrostatic field would diminish. Both the thickness and material of the coating will influence the frequency for maximum charge density. The insulation coating should be chosen with a relaxation time sufficiently similar to that of the continuous phase, so that any disturbance to coalescence will be minimum. The insulation also virtually cuts out all the field across the water–oil dispersion when d.c. is applied. Consequently, pulsed or a.c. fields must be used [23]. Practically, the coalescer depends for its application on the fact that even the best insulators are not totally devoid of conducting power [70].

7. Drop sizes

The size of droplets in emulsions may vary considerably in view of: (i) variation of interfacial properties (surfactant effects); (ii) variation in the water hold-up; (iii) variation in the level of shear to which the emulsion is subjected. Goto et al. [4] observed that the demulsification rate was apparently proportional to the square of the Sauter mean diameter. Hano et al. [33] reported the demulsification rate to be proportional to $d_{32}^{3.5}$ for a Span 80-kerosene organic phase. Williams and Bailey [10] used a laser light-scattering technique to look at the size distributions of water droplets in emulsions leaving an electrocoalescer. The volume median diameter was observed to increase with time, showing that drop–drop coalescence occurred in the emulsion. At low electric field strength, the drop size increase was small. Under a strong applied electric field, it increased very fast initially, but relatively slow after that. Therefore, coalescence effects attributed to sedimentation and Brownian motion are relatively insignificant compared to dipole and migratory coalescence produced in strong electric fields [10].

However, a water drop can be stretched in the direction of the applied field. The frequency of drop oscillation is twice the frequency of the sinusoidal alternating applied field [32]. An uncharged drop with radius r takes the shape of a prolate spheroid of eccentricity e, given by

$$e^2 = \frac{9\varepsilon\varepsilon_0 r E^2}{16\pi\lambda} \tag{7.1}$$

Williams et al. [38] and Urdahl et al. [88] found that even without an applied voltage the volume median diameter of suspended droplets increased at the coalescer outlet due to turbulent mixing (typically from 7 to 10 μm with their system). Droplet volume median diameter increased with the applied potential. However, at very high applied potential, the droplet size decreased as droplets broke up under electrostatic and hydrodynamic stresses [38].

Chen et al. [43] studied the coalescence time distribution of aqueous NaCl drops in n-heptane, and found that the average coalescence time was in the order of seconds for 3.60 mm diameter droplets. With the application of an electric field, the coalescence time could be reduced to well below 1 s. To predict the evolution of the drop-size distribution during a separation process, Zhang et al. [52] reported a population balance dynamics equation describing this distribution due to drop coalescence, provided by a mass conservation balance

$$\frac{\partial n_i}{\partial t} = \frac{1}{2}\sum_{j=1}^{i-1} J_{i-j,j} - \sum_{j=1}^{n} J_{i,j} \tag{7.2}$$

where $J_{i,j}$ is the rate of collision per unit volume of drops of size i with drops of size j.

The first term on the right-hand side of Eq. (7.2) is the formation rate of drops of size i by collisions of two smaller drops (the factor of $\frac{1}{2}$ is to avoid double counting), and the second term is the loss rate of drops of size i due to their collisions with other drops. This is restricted to binary interactions and coalescence in a homogenous suspension of conducting, spherical drops in an immiscible fluid. Changes in drop sizes are due to drop coalescence only, neglecting other effects such as drop dissolution, diffusion and break-up. The collision rate is given by Eq. (7.3):

$$J_{ij} = n_i n_j \pi (r_i + r_j)^2 |\underline{U}_i^{(0)} - \underline{U}_j^{(0)}| K_{\mathrm{c}} \tag{7.3}$$

where K_{c} is defined as the ratio of the actual collision rate to that for rectilinear drop motion due to gravity alone in the absence of drop–drop interactions. The collision efficiency describes effects of electric-field-induced forces, van der Waals attraction, and hydrodynamic interactions on drop collision and coalescence [52].

8. Residence time of a liquid mixture in an electrostatic coalescer

Bailes and Larkai [85] showed a relationship between linear emulsion velocity, electrode area and residence time of a liquid mixture for a constant coalescence parameter of 90%.

The residence time reduces linearly with increasing mixture velocity, while the effective electrode area for coalescence is directly proportional to the residence time due to the design of the system, giving the hydrodynamic limits for this electrocoalescer. Williams et al. [38] measured the effects of field exposure time on the volume median diameter of water droplets in oil, and concluded that the droplet diameter increases with the exposure time until a maximum diameter is reached.

Williams et al. [38] and Urdahl et al. [88] concluded that turbulent mixing can cause drop–drop coalescence even without an applied electric field. Under an electric field, drop–drop coalescence generally increases with increasing applied potential and residence time in the field. For emulsions in turbulent flow, drop–drop coalescence by an applied electric field is effective in just a few seconds. Significant droplet growth occurs if the residence time is sufficient [63].

Water drops do not coalesce spontaneously with their bulk phase, but rest at the interface for some time, which may vary between 0 and 30 s or more, depending on many factors such as temperature, drop size, the shape of the interface and the presence of impurities [59]. However, considerable coalescence occurs when a high potential is applied, and the emulsion settles more rapidly.

The primary drop usually coalesces with the bulk phase causing the formation of a smaller secondary droplet, which exists at the interface for a certain time before coalescing and giving rise to yet another droplet [48]. A thin film of oil entrapped between the primary drop and its bulk phase is responsible for the rest-time phenomenon. This film drains under gravity to a stage where very small disturbances are sufficient to cause distortion of the film leading to its rupture. Electric fields have a significant effect in promoting coalescence [59], presumably by creating large disturbances to the thin film. As the electric field strength E_0 is increased, a critical value is reached at which there is an abrupt reduction in the rest time, the rest time being rather insensitive to drop size changes. Rather surprisingly, the critical value of E_0 decreases as the emulsifier concentration increased [58]. Some curious transient effects have also been reported by Allan and Mason [58].

An estimate of the time for the evolution of the mean droplet size of an emulsion in an electric field can be obtained by examining a simple model, dealing with a mono-dispersed emulsion which retains its mono-disperse character by undergoing pairwise coalescence [42]. It consists of passing from N drops of radius r to $\frac{1}{2}N$ drops of radius $(2^{1/3}r)$. The evolution time is then determined by the solution of the equation governing the relative movement of two neighbouring drops. By using Stokes's formula for the drag on a spherical drop and the dipolar expression (3.19a) for the force between two drops on the same field line, Eq. (8.1) is obtained.

$$\frac{4\pi\eta_{\mathrm{c}} r\,\mathrm{d}r'}{\mathrm{d}t} = 2F = \frac{-48\pi\varepsilon\varepsilon_0 E_0^2 r^6}{r'^4} \tag{8.1}$$

Solving Eq. (8.1) yields Eq. (8.2):

$$t_1 = \frac{8}{15}\left[\frac{n_{\mathrm{c}}}{\varepsilon\varepsilon_0 E_0^2}\right]\left[\left(\frac{d_0}{2r}\right)^5 - 1\right] \tag{8.2}$$

Assuming an initial cubic lattice arrangement of the drops, the distance d_0 is given by $d_0/r = (4\pi/3\phi)^{1/3}$; with the time t_1 depending only on the volume fraction ϕ, as in Eq. (8.3) [42].

$$t_1 = \frac{8}{15}\frac{\eta_{\mathrm{c}}}{\varepsilon\varepsilon_0 E_0^2}\left[\left(\frac{\pi}{6\phi}\right)^{5/3} - 1\right] \tag{8.3}$$

Generally, the time evolution of a polydisperse emulsion can be modelled from Eq. (8.4) [89],

$$\begin{aligned}\frac{\mathrm{d}N(w,t)}{\mathrm{d}t} &= \frac{1}{2}\int_0^w K(w', w-w')N(w',t)N(w-w',t)\,\mathrm{d}w' \\ &\quad - \int_0^\infty K(w,w')N(w,t)N(w',t)\,\mathrm{d}w'\end{aligned} \tag{8.4}$$

which is equivalent to Eq. (7.2) due to Zhang et al. [52]. The first integral in Eq. (8.4) is the production rate of drops of volume w through coalescence of smaller droplets and the second integral is the rate at which these droplets disappear.

9. Effect of an electric field on the mean rest time of drops at an interface

For any given system, the 'rest time' (i.e. the interval between the arrival of the drop at the interface and its coalescence) has a wide range of values, influenced by temperature fluctuations, vibration and contamination [35,48,57,90]. For a given concentration of drops, increasing drop size causes an increase in the rest time, suggesting that the probability of coalescence falls off continuously with increasing surface separation. However, the mean rest time can be reduced by the increased rate of film thinning due to electrical attraction [90]. Eq. (9.1) was derived for the approach of a drop to a flat interface, where $-(\mathrm{d}h/\mathrm{d}t)$ is the rate of film thinning [58].

$$-\frac{\mathrm{d}h}{\mathrm{d}t} = \left[\frac{2}{3\pi\eta_{\mathrm{c}} r_{\mathrm{c}}^4}\right] F h^3 \tag{9.1}$$

Provided the deformed section of an interface is small, drainage between the interface and the drop of radius r is equivalent to drainage between equal drops of radius $2r$ [58]. The time-determining step of the whole coalescence process is the drainage of thin layer [48].

Several regimes of drainage may be distinguished, depending on the rigidity and mobility of the interfaces, with only one permitting an analytic solution namely that of rigid immobile interfaces [71]. Important regimes of deformed-drop drainage are those of immobile, partially mobile and fully mobile interfaces. The latter regime splits into two sub-regimes, depending on whether inertial or viscous forces are more significant here. Earlier models assumed the film to be a parallel-sided layer [71] while later models included the effects of interfacial deformation and film flow, with all the models assuming simple boundary conditions: either constant interaction force or constant approach velocity. However, in reality, both of them will vary during a collision [71].

If the viscosity of the dispersed phase is relatively insignificant, drainage is controlled by the resistance of the film to deformation and acceleration as in the partially mobile case [71]. The parallel-film model for fully mobile interfaces leads to the drainage relation given by Eqs. (9.2a) and (9.2b) [71]:

$$\frac{\mathrm{d}H}{\mathrm{d}t}=\left[\frac{\lambda}{3\eta_{\mathrm{c}}r}\left(\frac{\mathrm{d}H}{\mathrm{d}t}\right)_0\right]\exp\left(\frac{-12\eta_{\mathrm{c}}t}{\rho_{\mathrm{c}}a^2}\right)-\frac{\lambda}{3\eta_{\mathrm{c}}r} \tag{9.2a}$$

$$H=\tfrac{1}{2}\ln h \tag{9.2b}$$

In the viscous limit ($\eta_{\mathrm{c}}\to\infty$), this becomes Eq. (9.3):

$$-\frac{\mathrm{d}h}{\mathrm{d}t}=\frac{2\lambda h}{3\eta_{\mathrm{c}}r} \tag{9.3}$$

which represents the viscous resistance to squeezing between two lubricated bodies. Eq. (9.3) can be integrated to give Eq. (9.4).

$$h=h_0\exp\left(\frac{-t}{t_{\mathrm{ch}}}\right),\qquad \text{where}\qquad t_{\mathrm{ch}}=\frac{3\eta_{\mathrm{c}}r}{2\lambda} \tag{9.4}$$

In the inertia-controlled limit, Eq. (9.2a) reduces to Eq. (9.5a):

$$h=h_0\exp\left(\frac{-t}{t_{\mathrm{ch}}}\right) \tag{9.5a}$$

$$t_{\mathrm{ch}}=\frac{\rho VR^2}{8\sigma} \tag{9.5b}$$

According to Mohammed et al. [5], the demulsification rate is greatly influenced by the nature of the emulsion and the stage it has reached at some moment in time. In an electric field, there is an attractive force between the drop and the interface due to opposite charges which, as the film thins, may become much larger than the gravitational force, causing an increase in $-(\mathrm{d}h/\mathrm{d}t)$ and a decrease in the time required to drain the film to the critical thickness. The attractive force for a rigid conducting sphere near a grounded plane is given by Eq. (9.6).

$$F_{\mathrm{e}}=\varepsilon V_{\mathrm{s}}^2\psi_1\left(\frac{h}{b}\right) \tag{9.6a}$$

$$\psi_1\left(\frac{h}{b}\right)=\frac{1}{2}\sum_{n=0}^{\infty}\operatorname{cosec}(hn\omega)(\coth\omega-n\coth n\omega) \tag{9.6b}$$

$$\omega=\cosh^{-1}\left(\frac{h}{b}+1\right) \tag{9.6c}$$

Therefore, increasing the field strength at the interface has the effect of decreasing the mean rest time for a given drop size [36], and will eventually cause an instantaneous and single-staged drop coalescence. Brown and Hanson [59] also observed that increasing temperature produces a decrease in the rest time, because at higher temperatures the viscosity of the continuous phase will decrease, resulting in more rapid film thinning. The potential drop across the aqueous layer is relatively insignificant. Thus, it is the field strength at the interface that affects the coalescence rather than any induced charge on the drop itself [59].

10. Effect of hold-up fraction of dispersed phase and surface-active components on electrostatic coalescence

The influence of the hold-up of dispersed phase on drop–drop coalescence is notable at low applied voltages [36,40]. At an optimum pulse frequency and applied potential, the coalescence efficiency increases rapidly up to an aqueous hold-up of about 25% and then decreases slightly with larger hold-up, possibly due to changes in the mechanism of drop coalescence at this threshold value [40]. Bailes and Larkai [40] show that changing the hold-up should not affect the polarisation/relaxation characteristics of the system, which largely determines the optimum frequency.

Since the hold-up affects the size and number of drops in a dispersion, it will also affect the polarisation charge that can be induced on each drop for a given electric field and frequency. Hence the hold-up has an effect on the collision rate of the drops and the coalescence parameter. However, the demulsification rate is retarded after 60–70% demulsification, probably because the volume ratio of the continuous phase to that of the aqueous phase increases gradually, resulting in the decrease in effectiveness of the electric-induced force [36]. The effect of applied voltage decreases with higher flow rate as less time is available for the electric field to help bring adjacent droplets into close contact for electro-coalescence to occur [63]. Moreover, Sun et al. [3] reported that electric fields are ineffective for emulsions having a high water content because it can produce a ‘sponge’ phase which contains abundant aqueous phase at the water/oil interface.

Allan and Mason [58] observed that the addition of small amounts of surfactant in the heptane layer significantly increased the rest time of water drops at a water/heptane interface. The water drops were observed to have larger deformation at the interface due to decreased interfacial tension.

The increase in water-to-oil ratio reduces the average distance between water drops, and increases interfacial area between the oil and the dispersed phase [91,92], causing a decrease in density of surfactant at the interface [12]. Generally, the water/crude oil interfacial film properties significantly affect the separation efficiency [5,48]. An increase in surfactant concentration will decrease the demulsification rate [93,94] for several reasons as described below.

Emulsion formation can be caused by the surfactant-like action of polar compounds such as resins and asphaltenes in oil [11,66]. However, the kinetics and energy of formation of emulsions are still not clearly understood [95], as emulsions often form rapidly after the necessary chemical conditions and wave action or other turbulent energy input are achieved [91,94–96]. Crude oil indigenous solids and interfacially active components, notably wax crystallites, asphaltenes and resins, when present at the oil–water interface, may impart considerable stability [49,56,97] and rheological property changes to the emulsion [17,58,98,99]. Chen et al. [37] showed that the solid interfacial film is a key factor for the prevention of coalescence between droplets in an electric field, while Ese et al. [17] observed that stability also depends on the amount of asphaltenes, the degree of aging of asphaltenes and resins, and the ratio between asphaltenes and resins. Puskas et al. [97] established that a paraffin derivative of higher molar mass and melting point, containing polar end-groups, can also stabilise water-in-oil emulsions. However, it is not just the presence or absence of these solids which determine emulsion stability, but also the size of these solids in relation to that of the dispersed aqueous phase [100]. The effective viscosity of crude oil is also greatly increased following the dispersion of water to give a stable emulsion [11,36,49,97,101]. Hano et al. [33] investigated the effect of oil phase viscosity on demulsification rate, reporting that the demulsification rate is proportional to the -3.2 power of the oil phase viscosity. Goto et al. [4] then suggested that the empirical rate constant for coalescence should depend on the mean drop size and the viscosity of the continuous phase according to the following form:

$$K_{\mathrm{d}} = k' d_{32}^{3} \eta_{\mathrm{c}}^{-3.2} \tag{10.1}$$

However, many fundamental questions on stability mechanisms and destabilisation processes are still unresolved [48,94]. Fordedal et al. [11] and Mohammed et al. [66] who believed that the emulsion stability in crude oil systems is mainly controlled by the separated asphaltene fraction as far as the coalescence is concerned, revealed the importance of the interaction between asphaltenes and resins, by showing that the resins cannot alone stabilise w/o emulsions although the resins fraction might be even more interfacially active than the asphaltenes. Stronger interfacial film structures develop by increased packing and rearrangement of asphaltenes. The oil/water interfacial films show low viscosity initially. Due to the continuing in the adsorption of higher molecular weight species, the films build up, attaining a steady value for the interfacial tension after a period of hours [5].

Recently, interfacial properties of lipophilic, non-ionic surfactants of the sorbitan fatty acid ester type (Spans 20, 80, 83 and 85) have been investigated by Opawale and Burgess [82]. These surfactants, except Span 85, formed viscoelastic films at the water–oil interface, with multilayer formation for Spans 80 and 83. Surfactants which formed relatively strong interfacial films in the presence of common salt dissolved in the aqueous phase formed more stable emulsions [56,82]. Maximising the interfacial film strength by increasing surfactant concentration, using low or no salt content in the aqueous phase, and/or applying low temperature is likely to lead to the formation of more stable w/o emulsions using Spans 20, 80 and 83 [82].

11. Conclusions

The major mechanisms of electrocoalescence and separation, such as chain formation of droplets, dipole coalescence, dielectrophoresis, electrophoresis, random collisions and film drainage and rupture have been reviewed. The predominant mechanism in any system depends on electrode design and set-up, and emulsion properties, as well as on the type of electric field employed. For dipole coalescence to be effective, droplets have to be brought into close contact with each other. When the coalescence process is slow due to, e.g. interfacial phenomena, the droplets may form chains along the electric field direction, depending on the hydrodynamic conditions. This can produce a low resistance path for the electric current, leading to the electrical clamping at contact points between the droplets due to current constriction, which in turn can cause the rupture of the film between the droplets. In the extreme case, chains of aqueous droplets connecting the electrodes will create short-circuits, leading to collapse of the electric field. However, the role of electrical clamping phenomenon in electrocoalescence has not been widely investigated. The mechanism of film drainage and rupture is of paramount importance as it governs droplet–droplet and droplet–interface coalescence. However, the actual mechanisms underlying droplet–droplet coalescence are not yet fully understood.

Various mathematical models have been highlighted here, which depend on the mechanism and the type of electric field applied, such as population balance modelling, random collision/coalescence modelling, and linear condensation polymerisation kinetics. Factors influencing the coalescence efficiency have also been highlighted and reviewed. The several types of electric field which may be applied have been highlighted such as a.c., d.c. and pulsed d.c., as well as their combinations. The a.c. electric field is the oldest technique, with the current trend moving towards a pulsed d.c. electric field. The concept of an optimum applied frequency has been introduced together with that of a pulsed d.c. electric field, depending on the relaxation time of the various dielectrics, electrical properties of the continuous phase and the electrode coating material, and their thicknesses. In order to reduce the negative effect of electrode insulation, the dielectric properties of the insulation material should be similar to the continuous phase of the emulsion system.

Finally, the characteristics of the emulsion system itself determine the practicality of employing a strong electric field to break the emulsion. Emulsions with high aqueous-phase content will tend to short-circuit bare electrodes and cause the applied electric field to collapse, diminishing the coalescence efficiency which is one of the reasons for employing coated electrodes.

Investigations using crude oils are influenced by various unknown impurities and surface-active components in the system, making it difficult to interpret the causes and effects of various factors. Crude oil contains indigenous solids and interfacially active components, notably wax crystallites, asphaltenes and resins. When these compounds are present at the oil–water interface, they may impart considerable stability to the emulsion, as well as rheological property changes to the system. It has been shown that the solid interfacial film is a key factor in the prevention of coalescence between droplets in an electric field. Therefore, a fundamental understanding of the role of the impurities is highly desirable.

From this review paper, it has become clear that more investigations, both experimental and theoretical, are needed to study the electrocoalescence phenomenon at a microscopic level. This will help to elucidate the role of various parameters in the coalescence of two droplets, and between a droplet and an interface. This knowledge will then contribute to the design and operation of more efficient as well as more compact electrocoalescers.

Acknowledgements

One of the authors, JSE, would like to acknowledge the financial support of the Committee of Vice-Chancellors and Principals (CVCP) of the Universities of the United Kingdom, and the University of Surrey.

References

[1] R.A. Mohammed, A.I. Bailey, P.F. Luckham, S.E. Taylor, Dewatering of crude oil emulsions: 3. Emulsion resolution by chemical means, Colloids Surf. A 83 (1994) 261–271.

[2] K.J. Lissant, Demulsification: Industrial Application, Surfactant Science Series, Vol. 13, Marcel Dekker, New York, 1983.

[3] D. Sun, S.C. Jong, X.D. Duan, D. Zhou, Demulsification of water-in-oil emulsion by wetting coalescence materials in stirred- and packed-columns, Colloids Surf. A 150 (1999) 69–75.

[4] M. Goto, J. Irie, K. Kondo, F. Nakashio, Electrical demulsification of w/o emulsion by continuous tubular coalescer, J. Chem. Eng. Jpn. 22 (4) (1989) 401–406.

[5] R.A. Mohammed, A.I. Bailey, P.F. Luckham, S.E. Taylor, Dewatering of crude oil emulsions: 1. Rheological behaviour of the crude oil–water interface, Colloids Surf. A 80 (1993) 223–235.

[6] F.G. Cottrell, J.B. Speed, Separating and collecting particles of one liquid suspended in another liquid, US Patent 987,115 (1911).

[7] F.G. Cottrell, Process for separating and collecting particles of one liquid suspended in another liquid, US Patent 98,711,421 (1911).

[8] P.J. Bailes, S.K.L. Larkai, An experimental investigation into the use of high voltage d.c. fields for liquid phase separation, Trans. IChemE 59 (4) (1981) 229–237.

[9] P.J. Bailes, S.K.L. Larkai, Liquid phase separation in pulsed d.c. fields, Trans. IChemE 60 (2) (1982) 115–121.

[10] T.J. Williams, A.G. Bailey, Changes in the size distribution of a water-in-oil emulsion due to electric field induced coalescence, IEEE Trans. Ind. Appl. 1A–22 (3) (1986) 536–541.

[11] H. Fordedal, Y. Schildberg, J. Sjoblom, J.L. Volle, Crude oil emulsions in high electric fields as studied by dielectric spectroscopy: influence of interaction between commercial and indigenous surfactants, Colloids Surf. A 106 (1996) 33–47.

[12] D. Sun, X. Duan, W. Li, D. Zhou, Demulsification of water-in-oil emulsion by using porous glass membrane, J. Membrane Sci. 146 (1998) 65–72.

[13] H. Brandenberger, D. Nussli, V. Piech, F. Widmer, Monodisperse particle production: a method to prevent drop coalescence using electrostatic forces, J. Electrostatics 45 (1999) 227–238.

[14] A. Bhardwaj, S. Hartland, Kinetics of coalescence of water droplets in water-in-crude oil emulsions, J. Disp. Sci. Technol. 15 (2) (1994) 133–146.

[15] F. Groeneweg, W.G.M. Agterof, P. Jaeger, J.J.M. Janssen, J.A. Wieringa, J.K. Klahn, On the mechanism of the inversion of emulsions, Trans. IChemE 76 (A) (1998) 55–63.

[16] M. Frenkel, R. Shwartz, N. Garti, Turbidity measurements as a technique for evaluation of water-in-oil emulsion stability, J. Disp. Sci. Technol. 3 (2) (1982) 195–207.

[17] M. Ese, J. Sjoblom, H. Fordedal, O. Urdahl, H.P. Ronningsen, Ageing of interfacially active components and its effect on emulsion stability as studied by means of high voltage dielectric spectroscopy measurements, Colloids Surf. A 123–124 (1997) 225–232.

[18] C. Dalmazzone, H. Seris, Use of the DSC technique to characterize water-in-crude oil emulsions stability, Revue de l'Institut Francais du Petrole 53 (4) (1998) 463–464.

[19] J.C. Godfrey, M.J. Slater, Liquid–Liquid Extraction Equipment, Wiley, Chichester, UK, 1994.

[20] C.E. Figueroa, J.P. Wagner, A liquid membrane approach for removal of metallic species from resinous extracts under imposed electrical fields, Bioresour. Technol. 60 (1997) 153–160.

[21] G.E. Charles, S.G. Mason, The coalescence of liquid drops with flat liquid/liquid interfaces, J. Colloid Sci. 15 (1961) 236–267.

[22] H. Ino, N. Imaishi, M. Hozawa, K. Fujinawa, Demulsification of W/O emulsion under applied AC potential, Kagaku Kogaku Ronbunsyu 9 (1983) 263–269.

[23] C.P. Galvin, Design principles for electrical coalescers, IChemE Symp. Ser. 88 (1986) 101–113.

[24] M. Yamaguchi, A. Kobayashi, K. Ohbori, T. Katayama, A method of continuous phase separation of water in oil emulsion by applying d.c. electric field, Kagaku Kogaku Ronbunsyu 11 (1985) 729–734.

[25] E.C. Hsu, N.N. Li, Membrane recovery in liquid membrane separation processes, Sep. Sci. Technol. 20 (2–3) (1985) 115–130.

[26] A. Kriechbaumer, B. Marr, Emulsion breaking in electric fields, ACS Symp. Ser. (1985) 381–398.

[27] T. Kataoka, T. Nishiki, Experimental study of electrical demulsification in liquid surfactant membranes, Kagaku Kogaku Ronbunsyu 12 (1986) 16–22.

[28] Y. Mori, W. Eguchi, Coalescence of water-in-oil emulsion in a.c. high voltage field, Proc. World Cong. Chem. Eng. 3 (1986) 235–238.

[29] P.J. Bailes, E.H. Stitt, Column liquid contacting with vigorous agitation balanced by electrostatic coalescence, Chem. Eng. Res. Des. 65 (1987) 514–523.

[30] Z. Yan, S. Li, Y. Yu, X. Zheng, An investigation into the breaking-down of water-in-oil type emulsions by means of pulsed voltage, Desalination 62 (1987) 323–328.

[31] A. Kumar, F. Ansermet, S. Hartland, Influence de la coalescence electrostatique sur le debit d'une colonne d'extraction a melangeurs-decanteurs, Can. J. Chem. Eng. 65 (1987) 339–341.

[32] S.E. Taylor, Investigations into the electrical and coalescence behaviour of water-in-crude oil emulsions in high voltage gradients, Colloids Surf. 29 (1988) 29–51.

[33] T. Hano, T. Ohtake, K. Takagi, Demulsification kinetics of w/o emulsion in an a.c. electric field, J. Chem. Eng. Jpn. 21 (4) (1988) 345–351.

[34] H. Hauertmann, W. Degener, K. Schugerl, Electrostatic coalescence: reactor, process control, and important parameters, Sep. Sci. Technol. 24 (1989) 253–273.

[35] S.E. Taylor, Conductivity and coalescence of water-in-crude oil emulsions under high electric fields, Inst. Phys. Conf. Ser. 118 (3) (1991) 185–190.

[36] T. Hirato, K. Koyama, T. Tanaka, Y. Awakura, H. Majima, Demulsification of water-in-oil emulsion by an electrostatic coalescence method, Mater. Trans. JIM 32 (3) (1991) 257–263.

[37] T.Y. Chen, R.A. Mohammed, A.I. Bailey, P.F. Luckham, S.E. Taylor, Dewatering of crude oil emulsions 4. Emulsion resolution by the application of an electric field, Colloids Surf. A 83 (1994) 273–284.

[38] T.J. Williams, A.G. Bailey, M.T. Thew, The electrostatic destabilisation of water-in-oil emulsions in turbulent flow, Inst. Phys. Conf. Ser. 143 (1) (1995) 13–16.

[39] S.E. Taylor, Theory and practice of electrically enhanced phase separation of water-in-oil emulsions, Trans. IChemE 74 (A) (1996) 526–540.

[40] P.J. Bailes, S.K.L. Larkai, Influence of phase ratio on electrostatic coalescence of water/oil dispersions, Chem. Eng. Res. Des. 62 (1984) 33–38.

[41] E.E. Isaacs, R.S. Chow, Practical aspects of emulsion stability, Adv. Chem. Ser. 231 (1992) 251–277.

[42] P. Atten, Electrocoalescence of water droplets in an insulating liquid, J. Electrostatics 30 (1993) 259–270.

[43] C.T. Chen, J.R. Maa, Y.M. Yang, C.H. Chang, Effects of electrolytes and polarity of organic liquids on the coalescence of droplets at aqueous–organic interfaces, Surf. Sci. 406 (1998) 167–177.

[44] L.C. Waterman, Electrical coalescers, Chem. Eng. Prog. 61 (10) (1965) 51–57.

[45] A. Bleier, Colloids, in: Kirk-Othmer Encyclopedia of Chemical Technology, John Wiley & Sons, Inc. Vol. 6, 4th Edition, 1996, pp. 812–832.

[46] R. Clift, J.R. Grace, M.E. Weber, Bubbles, Drops, and Particles, Academic Press, New York, 1978.

[47] C.C. Man, A.W. Pacek, A.W. Nienow, Coalescence in dilute non-viscous liquid/liquid dispersions: numerical simulation and experimental results, IChemE Jubilee Res. Event (1997) 356–375.

[48] W. Rommel, W. Meon, E. Blass, Review: hydrodynamic modeling of droplet coalescence at liquid–liquid interfaces, Sep. Sci. Technol. 27 (2) (1992) 129–159.

[49] S.E. Friberg, S. Jones, Emulsions, in: Kirk-Othmer Encyclopedia of Chemical Technology, John Wiley & Sons, Inc. Vol. 9, 4th Edition, 1996, pp. 393–413.

[50] E.D. Manev, C.S. Vassilieff, I.B. Ivanov, Hydrodynamics of thin liquid films, Colloid Polym. Sci. 254 (1976) 99–102.

[51] H.A. Pohl, The motion and precipitation of suspensoids in divergent electric fields, J. Appl. Phys. 22 (7) (1951) 869–871.

[52] X. Zhang, O.A. Basaran, R.M. Wham, Theoretical prediction of electric field-enhanced coalescence of spherical drops, AIChE J. 41 (7) (1995) 1629–1639.

[53] M. Rigby, E.B. Smith, W.A. Wakeham, G.G. Maitland, The Forces Between Molecules, Oxford University Press, Oxford, 1986.

[54] J. Israelachvili, Intermolecular and Surface Forces, Academic Press, London, 1992.

[55] A. Vrij, Possible mechanism for the spontaneous rupture of thin free liquid films, Discuss. Faraday Soc. 42 (1966) 23–33.

[56] A. Kabalnov, Thermodynamic and theoretical aspects of emulsions and their stability, Curr. Opin. Colloid Interf. Sci. 3 (1998) 270–275.

[57] G.E. Charles, S.G. Mason, The mechanism of partial coalescence of liquid drops at liquid/liquid interfaces, J. Colloid Sci. 15 (1960) 105–122.

[58] R.S. Allan, S.G. Mason, Effects of electric fields on coalescence in liquid–liquid systems, Trans. Faraday Soc. 57 (1961) 2027–2040.

[59] A.H. Brown, C. Hanson, Effect of oscillating electric fields on coalescence in liquid–liquid systems, Trans. Faraday Soc. 61 (1965) 1754.

[60] P.J. Bailes, M. Kalbasi, Charge measurement and leakage for single droplets in a liquid–liquid system, J. Electrostatics 10 (1981) 81–88.

[61] R.S. Allan, S.G. Mason, Particle motions in sheared suspensions: XIV. Coalescence of liquid drops in electric and shear fields, J. Colloid Sci. 17 (1962) 383–408.

[62] D. Sartor, A laboratory investigation of collision efficiencies, coalescence and electrical charging of simulated cloud droplets, J. Meteorol. 11 (1954) 91–103.

[63] I.G. Harpur, N.J. Wayth, A.G. Bailey, M.T. Thew, T.J. Williams, O. Urdahl, Destabilisation of water-in-oil emulsions under the influence of an a.c. electric field: experimental assessment of performance, J. Electrostatics 40–41 (1997) 135–140.

[64] C.A.R. Pearce, The mechanism of the resolution of water-in-oil emulsions by electrical treatment, Brit. J. Appl. Phys. 5 (1954) 136–143.

[65] C. Bezemer, C.A. Goes, Motion of water droplets of an emulsion in a non-uniform field, Brit. J. Appl. Phys. 6 (1955) 224–225.

[66] R.A. Mohammed, A.I. Bailey, P.F. Luckham, S.E. Taylor, Dewatering of crude oil emulsions 2. Interfacial properties of the asphaltic constituents of crude oil, Colloids Surf. A 80 (1993) 237–242.

[67] W.A. McRae, Electrophoresis, in: Kirk-Othmer Encyclopedia of Chemical Technology, John Wiley & Sons, Inc. Vol. 9, 4th Edition, 1996, pp. 356–375.

[68] H.A. Pohl, Some effects of nonuniform fields on dielectrics, J. Appl. Phys. 29 (8) (1958) 1182–1188.

[69] F.M. Joos, R.W.L. Snaddon, On the frequency dependence of electrically enhanced emulsion separation, Chem. Eng. Res. Des. 63 (1985) 305–311.

[70] P.J. Bailes, An electrical model for coalescers that employ pulsed d.c. fields, Trans. IChemE 73 (A) (1995) 559–566.

[71] A.K. Chesters, The modelling of coalescence processes in fluid–liquid dispersions: a review of current understanding, Trans. IChemE 69 (A) (1991) 259–270.

[72] D.J. Klingenberg, F. van Swol, C.F. Zukoski, Dynamic simulation of electrorheological suspensions, J. Chem. Phys. 91 (12) (1989) 7888–7895.

[73] W.R. Smythe, Static and Dynamic Electricity, 3rd Edition, McGraw-Hill, New York, 1968.

[74] R.B. Bird, W.E. Stewart, E.N. Lightfoot, Transport Phenomena, Wiley, New York, 1960.

[75] M.H. Davis, Two charged spherical conductors in a uniform electric field: forces and field strength, Quart. J. Mech. Appl. Math. 17 (1964) 499.

[76] M.J. Miksis, Shape of a drop in an electric field, Phys. Fluids 24 (11) (1981) 1967–1972.

[77] T. Nishiwaki, K. Adachi, T. Kotaka, Deformation of viscous droplets in an electric field: poly(propylene oxide)/poly(dimethylsilone) systems, Langmuir 4 (1988) 170–175.

[78] G. Taylor, Disintegration of water drops in an electric field, Proc. R. Soc. A 280 (1964) 383–397.

[79] Z. Krasucki, High-field conduction in liquid dielectrics, ACTES Coll. Int. No. 179, CNRS, 1968, pp. 311–323.

[80] P.J. Bailes, Electrically augmented settlers and coalescers for solvent extraction, Hydrometallurgy 30 (1–3) (1992) 417–430.

[81] J.D. Winslow Jr., Electrical treater with a.c.–d.c. electrical fields, US Patent 4,049,535 (1977).

[82] F.O. Opawale, D.J. Burgess, Influence of interfacial properties of lipophilic surfactants on water-in-oil emulsion stability, J. Colloid Interf. Sci. 197 (1998) 142–150.

[83] T. Hanai, Theory of the dielectric dispersion due to the interfacial polarization and its application to emulsions, Kolloid-Zeitschrift 171 (1960) 23–31.

[84] P.J. Bailes, P.D. Dowling, The production of pulsed E.H.T. voltages for electrostatic coalescence, J. Electrostatics 17 (3) (1985) 321–328.

[85] P.J. Bailes, S.K.L. Larkai, Polarisation effects in liquid phase separation by pulsed electric fields, IChemE Symp. Ser. 94 (1984) 235–245.

[86] I. Abou-Nemeh, M. Moors, A.P. van Peteghem, Electrostatic splitting of the emulsion used in liquid surfactant membranes process of metals separation, Sep. Sci. Technol. 27 (1992) 1319.

[87] E.C. Hsu, N.N. Li, T. Hucal, Electrodes for electrical coalescence of liquid emulsions, US Patent 4,415,426 (1983).

[88] O. Urdahl, T.J. Williams, A.G. Bailey, M.T. Thew, Electrostatic destabilization of water-in-oil emulsions under conditions of turbulent flow, Trans. IChemE 74 (A) (1996) 158–165.

[89] S.E. Sadek, C.D. Hendricks, Electrical coalescence of water droplets in low-conductivity oils, Ind. Eng. Chem. Fundam. 13 (1974) 139–142.

[90] G.A.H. Elton, R.G. Picknett, The coalescence of aqueous droplets with an oil/water interface, Proc. Int. Cong. Surf. Activity B (1957) 288–294.

[91] Th.F. Tadros, Fundamental principles of emulsion rheology and their applications, Colloids Surf. A 91 (1994) 39–55.

[92] M. Benayoune, L. Khezzar, M. Al-Rumhy, Viscosity of water in oil emulsions, Petroleum Sci. Technol. 16 (7–8) (1998) 767–784.

[93] F. Villamagna, M.A. Whitehead, A.K. Chattopadhyay, Mobility of surfactants at the water-in-oil emulsion interface, J. Disp. Sci. Technol. 16 (2) (1995) 105–114.

[94] J. Sjoblom, O. Urdahl, H. Hoiland, A.A. Christy, E.J. Johansen, Water-in-crude oil emulsion: formation, characterization, and destabilization, Prog. Colloid Polym. Sci. 82 (1990) 131–139.

[95] M. Fingas, Water-in-oil emulsion formation: a review of physics and mathematical modelling, Spill Sci. Technol. Bull. 2 (1) (1995) 55–59.

[96] R.D. Nelson Jr., Powders handling — dispersion of powders in liquids, in: Kirk-Othmer Encyclopedia of Chemical Technology, John Wiley & Sons, Inc. Vol. 19, 4th Edition, 1996, pp. 1093–1112.

[97] S. Puskas, J. Balazs, A. Farkas, I. Regdon, O. Berkesi, I. Dekany, The significance of colloidal hydrocarbons in crude oil production, Part 1. New aspects of the stability and rheological properties of water–crude oil emulsions, Colloids Surf. A 113 (1996) 279–293.

[98] D.G. Thompson, A.S. Taylor, D.E. Graham, Emulsification and demulsification related to crude oil production, Colloids Surf. 15 (1985) 175–189.

[99] A.B. Nordvik, J.L. Simmons, K.R. Bitting, A. Lewis, T. Strom-Kristiansen, Oil and water separation in marine oil spill clean-up operations, Spill Sci. Technol. Bull. 3 (3) (1996) 107–122.

[100] Y. Schildberg, J. Sjoblom, A.A. Christy, Characterization of interfacially active fractions and their relations to water-in-oil emulsion stability, J. Disp. Sci. Technol. 16 (7) (1995) 575–605.

[101] A.E. Omar, S.M. Desouky, B. Karama, Rheological characteristics of Saudi crude oil emulsions, J. Petroleum Sci. Eng. 6 (1991) 149–160.